

## INFORMATION TO USERS

This manuscript has been reproduced from the microfilm master. UMI films the text directly from the original or copy submitted. Thus, some thesis and dissertation copies are in typewriter face, while others may be from any type of computer printer.

**The quality of this reproduction is dependent upon the quality of the copy submitted.** Broken or indistinct print, colored or poor quality illustrations and photographs, print bleedthrough, substandard margins, and improper alignment can adversely affect reproduction.

In the unlikely event that the author did not send UMI a complete manuscript and there are missing pages, these will be noted. Also, if unauthorized copyright material had to be removed, a note will indicate the deletion.

Oversize materials (e.g., maps, drawings, charts) are reproduced by sectioning the original, beginning at the upper left-hand corner and continuing from left to right in equal sections with small overlaps.

ProQuest Information and Learning  
300 North Zeeb Road, Ann Arbor, MI 48106-1346 USA  
800-521-0600

UMI<sup>®</sup>





Université d'Ottawa · University of Ottawa



# CISPLATIN-INDUCED CYTOTOXICITY IN MDCK CELLS

By

Yan Julia Li

This thesis is submitted in partial fulfillment  
of the M.Sc. program in Pharmacology

Cancer Care Ontario  
Ottawa Regional Cancer Centre  
503 Smyth Road  
Ottawa, Ontario K1H 1C4  
Canada

&

Cellular and Molecular Medicine  
Faculty of Medicine, University of Ottawa  
451 Smyth Road  
Ottawa, Ontario K1H 8M5  
Canada

December, 12, 2001

Copyright© Yan Julia Li, Ottawa, Canada, 2001



National Library  
of Canada

Acquisitions and  
Bibliographic Services

395 Wellington Street  
Ottawa ON K1A 0N4  
Canada

Bibliothèque nationale  
du Canada

Acquisitions et  
services bibliographiques

395, rue Wellington  
Ottawa ON K1A 0N4  
Canada

*Your file Votre référence*

*Our file Notre référence*

The author has granted a non-exclusive licence allowing the National Library of Canada to reproduce, loan, distribute or sell copies of this thesis in microform, paper or electronic formats.

The author retains ownership of the copyright in this thesis. Neither the thesis nor substantial extracts from it may be printed or otherwise reproduced without the author's permission.

L'auteur a accordé une licence non exclusive permettant à la Bibliothèque nationale du Canada de reproduire, prêter, distribuer ou vendre des copies de cette thèse sous la forme de microfiche/film, de reproduction sur papier ou sur format électronique.

L'auteur conserve la propriété du droit d'auteur qui protège cette thèse. Ni la thèse ni des extraits substantiels de celle-ci ne doivent être imprimés ou autrement reproduits sans son autorisation.

0-612-72777-7

## ABSTRACT

Background: The mechanism of cisplatin-induced nephrotoxicity is not well understood. The distal tubules are affected in both human and animal studies, although the majority of cisplatin-induced renal damage is in proximal tubules. Platinum (Pt) forms intra- and interstrand cross-links with DNA in cancer cells. Although the majority of Pt cross-links are intrastrand, both types of cross-links have been implicated in causing cisplatin-induced cytotoxicity in cancer cells. Hypothesis: A mechanism of cisplatin-induced cytotoxicity in MDCK cells relates to its ability to bind to DNA and interfere with its synthesis. Methods: The canine distal renal tubular epithelial cell line, MDCK was used as an *in vitro* model to investigate the mechanism of cisplatin-induced nephrotoxicity. The intracellular Pt accumulation and Pt binding with DNA were assayed by atomic absorption spectrophotometry. DNA synthesis was measured by BrdU labeling and fluorescence microscopy at the concentrations from 0 to 100  $\mu\text{M}$ . The alkaline comet assay with 10 Gy radiation was used to measure Pt DNA interstrand cross-links after a one hour cisplatin exposure from 0 to 100  $\mu\text{M}$  at both zero and sixteen hour time points. According to the principles of alkaline comet assay, the tail moment is inversely related with the amount of Pt interstrand cross-links. Results: The doubling time of MDCK cells was  $40 \pm 5$  hours (SD) (n=3). The plating efficiency of MDCK cells was  $16 \pm 3\%$  (SD) (n=4). The  $\text{IC}_{50}$  of cisplatin after a one hour exposure was  $17 \pm 5$   $\mu\text{M}$  (SD) (n=4). Platinum binding with DNA is proportional with cisplatin exposure concentrations at the supra-cytotoxicity range (i.e. cisplatin concentrations higher than those used in clonogenic assay). When cells were exposed to 1.5 mM cisplatin for one hour, the amount of platinum binding with DNA was  $0.24 \pm 0.04$  ng platinum per  $\mu\text{g}$  of DNA (SD)

(n=3). DNA synthesis was significantly inhibited after a one hour cisplatin exposure as measured by the method of BrdU microscopy. At the exposure concentration of 25  $\mu\text{M}$ , DNA synthesis was significantly inhibited by  $40\pm 4\%$  (SD) (n=3) ( $p < 0.001$ ) compared to control. The alkaline comet assay detected that platinum formed interstrand cross-links with DNA after a one hour cisplatin exposure at both the zero and sixteen hour time points at the concentrations ranging from 5  $\mu\text{M}$  to 100  $\mu\text{M}$ . For example, at the exposure concentration of 25  $\mu\text{M}$ , the tail moment was reduced by  $20\pm 5\%$  (SD) (n=3) ( $p < 0.01$ ) compared with the control at the zero time point. The reduction of the tail moment has a strong correlation with the inhibition of DNA synthesis ( $r^2 = 0.95$ ) and with the cell survival ( $r^2 = 0.84$ ) for the zero time point, respectively. Conclusion: Platinum binding with DNA, forming interstrand cross-links and interfering with its synthesis is a process that may contribute to mechanism of cisplatin-induced cytotoxicity in MDCK cells.

## ACKNOWLEDGEMENTS

I would like to express my deepest appreciation to my supervisor Dr. Rakesh Goel, for his knowledge, advice, guidance, support and kindness. As well, I very much appreciate Dr. David Stewart for his support, generosity, and kindness during my education. I would also like to express my special appreciation to Dr. Douglas Franks, for his encouragement, patience, and kindness.

I am grateful to Dr. Srabani Banerjee as the previous manager of the pharmacology research laboratory for her technical assistance.

I would like to thank Dr. Ruth Wilkins and her colleagues in Health Canada; they supervised me in conducting comet assay and allowed me to use their equipment.

These are my special thanks to Dr. Michael McBurney and his staff in Ottawa Regional Cancer Centre Research Group, for their advice to my research project and allowing me to share their equipment with them.

Finally, I would like to thank all of my friends who helped me in the past, and those to whom this thesis is dedicated, my parents for their advice, support and encouragement throughout my life.

## TABLE OF CONTENTS

<b>Abstract.....</b>	<b>ii</b>
<b>Acknowledgements.....</b>	<b>iv</b>
<b>Table of Contents.....</b>	<b>v</b>
<b>List of Figures.....</b>	<b>viii</b>
<b>List of Tables.....</b>	<b>x</b>
<b>List of Abbreviations.....</b>	<b>xi</b>
<b>1. Introduction.....</b>	<b>1</b>
1.1 History.....	1
1.2 Chemistry.....	4
1.3 Chemical Reactions.....	4
<i>1.3.1 Stability and Hydrolysis.....</i>	<i>4</i>
<i>1.3.2 Reactions with DNA.....</i>	<i>7</i>
<i>1.3.3 Binding Modes of Cisplatin with DNA.....</i>	<i>9</i>
1.3.3.1 Intrastrand Cross-links.....	10
1.3.3.2 Interstrand Cross-links.....	10
1.3.3.3 DNA-protein Cross-links.....	11
1.4 Pharmacology.....	13
<i>1.4.1 Clinical Applications.....</i>	<i>13</i>
<i>1.4.2 Pharmacokinetics.....</i>	<i>13</i>
1.4.2.1 General Parameters.....	13
1.4.2.2 Cell Membrane Transport.....	14
<i>1.4.3 Mechanism of Action.....</i>	<i>15</i>

1.4.3.1 DNA Interaction.....	15
1.4.3.2 Cisplatin-induced Cell Death.....	15
1.5 Toxicology.....	16
1.5.1 Cisplatin-induced Clinical Side Effects.....	16
1.5.2 Cisplatin-induced Nephrotoxicity .....	17
1.5.2.1 Pre-clinical Studies .....	17
1.5.2.2 Clinical Studies.....	18
1.6 The Strength and Weakness of the Current Knowledge.....	20
1.7 Hypothesis and Specific Aims for This Project.....	22
1.7.1 Hypothesis.....	22
1.7.2 Specific Aims of This Project.....	22
<b>2. Materials and Methods.....</b>	<b>23</b>
2.1 Cell Line.....	23
2.2 Methodology to be Used for This Project.....	24
2.3 Growth Curve of MDCK Cells .....	25
2.3.1 Materials.....	25
2.3.2 Methods.....	26
2.4 Cisplatin-induced Cytotoxicity.....	27
2.4.1 Materials.....	27
2.4.2 Methods.....	27
2.5 Cellular Accumulation of Platinum.....	28
2.5.1 Atomic absorption.....	28
2.5.2 Materials.....	32
2.5.3 Methods.....	32

2.6 Platinum Binding with DNA.....	34
2.6.1 <i>Materials</i> .....	34
2.6.2 <i>Methods</i> .....	35
2.7 Cisplatin-induced DNA Synthesis Inhibition.....	37
2.7.1 <i>Background</i> .....	37
2.7.2 <i>Materials</i> .....	39
2.7.3 <i>Methods</i> .....	40
2.8 Cisplatin-induced Pt-DNA Interstrand Cross-links.....	41
2.8.1 <i>Background</i> .....	41
2.8.2 <i>Materials</i> .....	45
2.8.3 <i>Methods</i> .....	47
<b>3. Results.....</b>	<b>50</b>
3.1 Growth Curve of MDCK cells.....	50
3.2 Cisplatin-induced Cytotoxicity Measurement.....	52
3.3 Cellular Accumulation of Platinum.....	54
3.4 Platinum Binding with DNA.....	56
3.5 Cisplatin-induced DNA Synthesis Inhibition.....	58
3.6 Cisplatin-induced Pt-DNA Interstrand Cross-links.....	62
<b>4. Discussion.....</b>	<b>72</b>
<b>5. References.....</b>	<b>77</b>

## LIST OF FIGURES

Figure 1.1: Chemical structure of cisplatin.....	3
Figure 1.2a: The first two steps of cisplatin hydrolysis .....	6
Figure 1.2b: The complete hydrolysis of cisplatin.....	6
Figure 1.3: Functional binding modes of cisplatin with DNA.....	12
Figure 1.4: DNA-protein cross-link.....	12
Figure 3.1: Growth curve of MDCK cells.....	51
Figure 3.2: Cisplatin dose-response curve.....	53
Figure 3.3: Regression curve of platinum accumulation in MDCK cells after a one hour exposure.....	55
Figure 3.4: Regression curve of platinum binding with DNA versus corresponding cisplatin exposure concentrations.....	57
Figure 3.5: Fluorescence microscopy of MDCK cells.....	59
Figure 3.6: Percentage of cells labeled with BrdU after a one hour cisplatin exposure...	60
Figure 3.7: Correlation of percentage of cells labeled with BrdU and cell survival.....	61
Figure 3.8: Reduction of tail moment after a one hour cisplatin exposure at zero and sixteen hour time points.....	65
Figure 3.9: Correlation of percentage of cells labeled with BrdU and percentage of tail moment at zero hour time point.....	67
Figure 3.10: Correlation between percentage of cell survival and percentage of tail moment at zero hour time point after a one hour cisplatin exposure.....	68
Figure 3.11: Correlation between percentage of cell survival and percentage of tail moment at sixteen hour time point after a one hour cisplatin exposure.....	69

Figure 3.12: Image of the “comet” of individual lysed cells after alkaline comet assay at zero hour time point.....70

Figure 3.13: Image of the “comet” of individual lysed cells after alkaline comet assay at sixteen hour time point.....71

## LIST OF TABLES

Table 2.1: Furnace operating parameter for the measurements of Pt in a cell suspension sample.....	31
Table 2.2: Parameters of Pt assay by atomic absorption spectrophotometry.....	31
Table 3.1: The comparison of the percentage of tail moment at the one hour and sixteen hour time points.....	66

## LIST OF ABBREVIATIONS

ATCC	American Type Culture Collection
AA	Atomic absorption
BUN	Blood urea nitrogen
DNA	Deoxyribonucleic acid
FBS	Fetal bovine serum
GFR	Glomerular filtration rate
MDCK	Madin-Darby canine kidney
MGE	Micro gel electrophoresis
PBS	Phosphate buffered saline
Pt	Platinum
RNA	Ribonucleic acid
SD	Standard deviation
SCr	Serum creatinine
SCGE	Single cell gel electrophoresis assay
SCG	Single cell gel assay

# 1. Introduction

## 1.1 History:

As an anticancer drug, cisplatin (*cis*-diamminedichloroplatinum) has been used for a variety of cancers, including ovarian cancer, testicular cancer, lung cancer, etc. (Salmon et al., 1995). In the early 1960s, Barnett Rosenberg and his colleagues observed an interesting phenomenon during a study, which examined bacterial growth in an electric field. *Escherichia coli* bacteria were grown in a chamber containing ammonium chloride as the nitrogenous source, while the current was passed through the bacteria by a set of platinum electrodes. It was observed that bacterial growth was filamentous and this appeared to be influenced by the current. Bacterial rods formed strands 300 times longer than their usual length of 2-5  $\mu\text{m}$ . Cell division was suppressed without causing bacterial death (Rosenberg et al., 1965).

During further investigation, it was discovered that the filamentous growth of the bacteria was caused by platinum dissolved in the ammonium chloride solution from the electrodes, but not the current. Initially, the chemical was defined as *cis*-[Pt(NH<sub>3</sub>)<sub>2</sub>Cl<sub>4</sub>]. Following subsequent studies of the effects of a group of other platinum compounds on the filamentous growth of the bacteria, the divalent compound *cis*-[Pt(NH<sub>3</sub>)<sub>2</sub>Cl<sub>2</sub>] was found to actively suppress bacterial growth, but this was not observed with the trans isomer (Rosenberg et al., 1967).

Since the solution of *cis*-[Pt(NH<sub>3</sub>)<sub>2</sub>Cl<sub>4</sub>] inhibited cell division without killing the cell, it was conjectured that these compounds may halt the rapid growth of tumor cells

without causing severe toxicity to the host animal. *Cis*-[Pt(NH<sub>3</sub>)<sub>2</sub>Cl<sub>2</sub>] and *cis*-[Pt(NH<sub>3</sub>)<sub>2</sub>Cl<sub>4</sub>] were tested against Sarcoma 180 in mice and were found to be effective in suppressing tumor growth (Rosenberg, 1970). The above *cis* isomers of the platinum compounds were then submitted to the U.S. National Cancer Institute for further analysis; they were tested against L1210 leukemia in mice. These two compounds were observed to have potent anti-tumor activity. Rosenberg and VanCamp discovered that *cis*-[Pt(NH<sub>3</sub>)<sub>2</sub>Cl<sub>2</sub>] was effective in regression of large solid Sarcoma 180 tumors (8 days old) in Swiss white mice (Rosenberg, 1970). *Cis*-[Pt(NH<sub>3</sub>)<sub>2</sub>Cl<sub>2</sub>] (Figure 1.1) appeared to be more potent against a variety of animal transplanted tumors. Extensive toxicological and clinical trials ensued in 1972; cisplatin was approved for clinical use by the FDA in 1979 (Sherman et al., 1987).

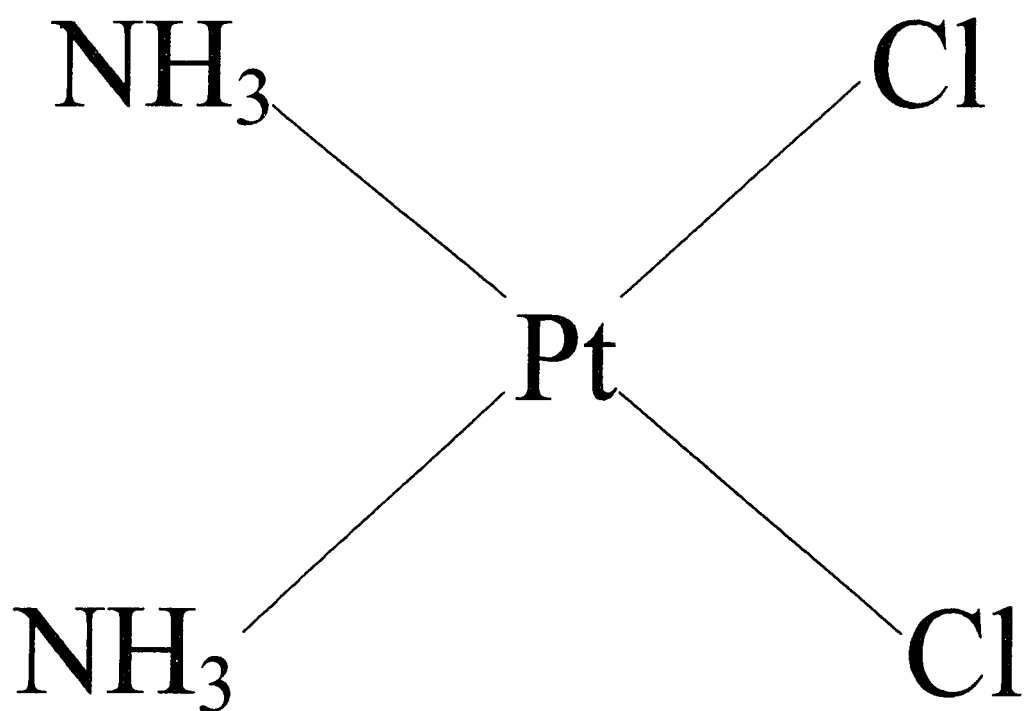


Figure 1. 1 Chemical structure of cisplatin

## 1.2 Chemistry:

Both stereoisomers of diamminedichloroplatinum (II) have two chloride ligands and two ammine ligands, but only the *cis* isomer displays the anticancer activity (Sherman et al., 1987). The *trans* isomer was found to be more reactive in chemical reactions than the *cis* analog. *Trans*-[Pt(NH<sub>3</sub>)<sub>2</sub>Cl<sub>2</sub>] aquates four times faster than *cis*-[Pt(NH<sub>3</sub>)<sub>2</sub>Cl<sub>2</sub>] (Tucker et al., 1964). The *trans* isomer tends to react more quickly with various body constituents and with less specificity during chemical reactions than the *cis* compound (Hoeschele et al., 1971). Only the *cis* compound has the potential to form chelates, and it is possible that the anticancer activity is largely associated with a chelating interaction. Chemical studies have demonstrated that chlorides are the reactive ligands, while Pt-NH<sub>3</sub> bonds are very stable (Basolo et al., 1967).

## 1.3 Chemical Reactions:

### 1.3.1 Stability and Hydrolysis:

Cisplatin is an inorganic compound, which has planar geometry. As previously described, the chloride ligand is relatively labile while the Pt-NH<sub>3</sub> bond is more stable when cisplatin undergoes hydrolysis in water. The two chlorides are replaced by OH, and form aquated cisplatin (Figure 1.2b). The first two steps of hydrolysis are described in

Figure 1.2a and the complete hydrolysis of cisplatin in water is described in Figure 1.2b (Johnson et al., 2001) (Miller et al., 1991).

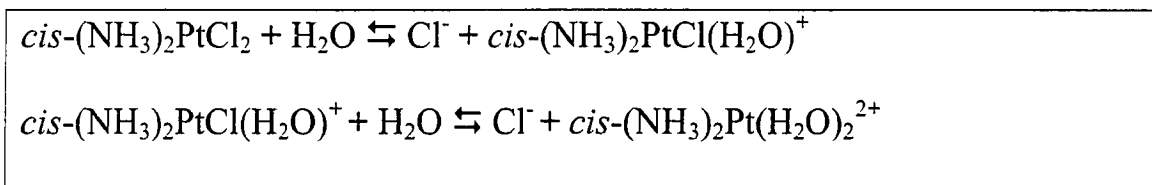


Figure 1.2a The first two steps of hydrolysis of cisplatin in water

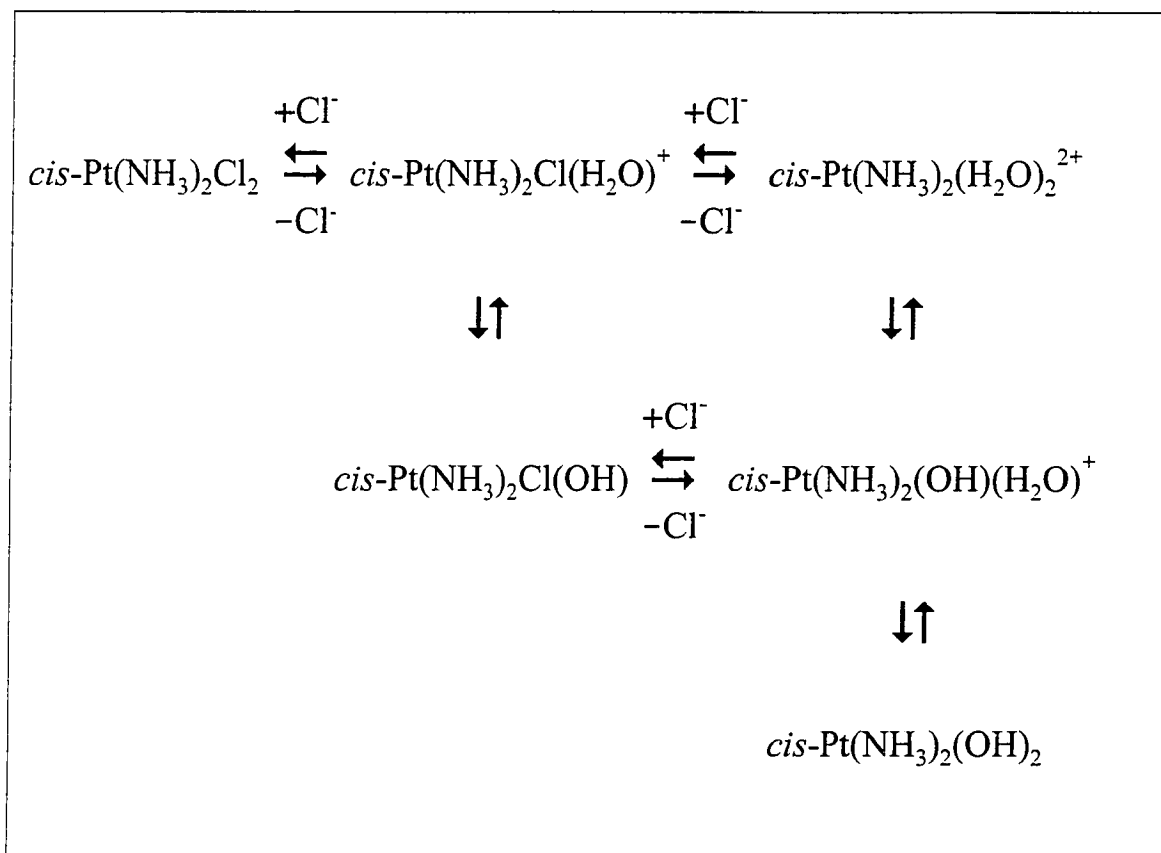


Figure 1. 2b The complete hydrolysis of cisplatin in water

Cisplatin achieves its highest stability in 0.9% sodium chloride. The maximal solubility of cisplatin in 0.9% saline is 1 mg/ml. The above cisplatin solution (1 mg/ml) is stable for approximately one year, when this solution is stored at room temperature between 15 to 25 °C in the dark (Faulding Canada Inc., Vaudreuil, QC, Canada).

### **1.3.2 Reactions with DNA**

Heavy metals may bind to numerous potential cellular components. The initial challenge for researchers was to determine the major cellular target of cisplatin for the anti-tumor activity (Sherman et al., 1987).

Cisplatin induced filamentous growth in bacteria, which meant that it inhibited cell division but without having simultaneously inhibited cell growth. Since some other agents, such as UV radiation or hydroxyurea, produce similar effects by inhibiting DNA synthesis, it was suggested that a similar mechanism might also apply to cisplatin's anti-tumor activity. The hypothesis was tested by measuring the rate of synthesis of DNA, RNA, and protein in both human AV<sub>3</sub> (human amnion) cells *in vitro*, and Ehrlich ascites tumor cells treated with cisplatin. At the therapeutic dose of cisplatin, DNA synthesis was preferentially inhibited compared with RNA and protein, in both human AV<sub>3</sub> cells *in vitro*, and Ehrlich ascites tumor cells *in vivo*. Synthesis of DNA, RNA and proteins in Ehrlich ascites tumor cells was measured *in vitro* at various intervals up to 96 hours after injection of cisplatin into mice. The incorporation rate of radiolabeled uridine and L-leucine into RNA and protein began to recover at 12-24 hours following the injection of

cisplatin. Restoration to normal synthesis of RNA and protein was virtually complete after 72-96 hours. In contrast, the incorporation rate of radiolabeled thymidine into DNA was persistently suppressed over the same time period studied. These results suggested that DNA is the major target, and the inactivation of DNA synthesis is mainly responsible for cisplatin's anti-tumor activity. Particularly, cisplatin is thought to bind with DNA directly, and render it unsuitable as a template for replication (Sherman et al., 1987).

Cisplatin is relatively stable in an aqueous environment such as blood plasma, where the chloride concentration is greater than 100 mM (O'Dwyer et al., 1996). The generally accepted mechanism of cisplatin interaction with DNA is stated as following. After clinical administration, the parental drug enters the blood stream. In plasma, where the chloride ion concentration (about 103 mM) is relatively higher than what is found intracellularly, the predominant species (the neutral dichloro complex) can cross cell membranes. Inside the cell, where the chloride ion concentration drops to about 4 mM, cisplatin loses its chloride atoms and is converted into an aquated reactive electrophile that can bind covalently to a variety of macromolecules including DNA. According to the early studies, the positively charged platinum complex may be electrostatically attracted to the negatively charged DNA (Sherman et al., 1987). Based on the recent studies of the reactions of cisplatin metabolism, the predominant species that react with DNA are likely to be the hydroxo aqua as well as chloro aqua species, which are described in Figure 1.2a and Figure 1.2b (Johnson et al., 2001). It has been suggested that cisplatin's anti-tumor activity may be related to its ability to cause lesions in DNA by forming DNA cross-links (Eastman A. et al., 1987).

### 1.3.3 Binding Modes of Cisplatin with DNA

There are a variety of binding sites available for heavy metals on DNA. Metals may covalently bind to the negatively charged phosphate oxygen atoms and to the nitrogen and oxygen atoms of the purine and pyrimidine bases. Planar molecules can intercalate between DNA base pairs (Sherman et al., 1987).

Early studies indicated that platinum binding to DNA is at the level of the nucleotide base (Sherman et al., 1987). Cisplatin reacts preferentially at the N7 position of guanine and adenine to form a variety of monofunctional and bifunctional adducts. The first step of the reaction involves the formation of monoadducts. These monoadducts may then react further to form intrastrand or interstrand cross-links. The predominant bidentate lesions that are formed with DNA *in vitro* are intrastrand cross-links. Cisplatin also forms interstrand cross-links between guanine residues located on opposite strands. These interstrand cross-links may contribute to cisplatin's cytotoxicity, because they impede certain cellular processes that require the separation of both DNA strands, such as replication and transcription (Johnson et al., 2001).

The monofunctional adducts formed by cisplatin are not considered to be responsible for cisplatin's biological activity. The bifunctional binding to two sites on a single base, cross-links between two bases on opposite strands of the DNA helix (interstrand cross-links), and cross-links between two bases on the same DNA strand (intrastrand cross-links) have all been proposed to be responsible for the anti-tumor activity of cisplatin (Sherman et al., 1987).

### 1.3.3.1 Intrastrand Cross-links

Intrastrand cross-links formed by cisplatin with DNA at N7 atoms of two adjacent guanosine nucleosides constitute the majority of all adducts both *in vivo* and *in vitro* (see Figure 1.3) (Sherman et al., 1987). The predominant bidentate lesions that are formed with DNA in cultured cells are the d(GpG)Pt, d(ApG)Pt, and d(GpNpG)Pt intrastrand cross-links. In a study of cisplatin treated Chinese hamster ovary (CHO) cells, these lesions were determined to account for approximately 60%, 15%, and 20% of the total platinum DNA adducts, respectively (Johnson et al., 2001). The formation of platinum DNA (Pt-DNA) intrastrand cross-links is repairable. The repair mechanism involves excision, re-synthesis of DNA by a DNA polymerase and the welding repair by ligase (Gellert et al., 1979). Platinum induced d(GpG) intrastrand cross-links are an important aspect of the cisplatin interaction with its biological target and are possibly a critical lesion responsible for its antitumor ability (Lippard, 1982).

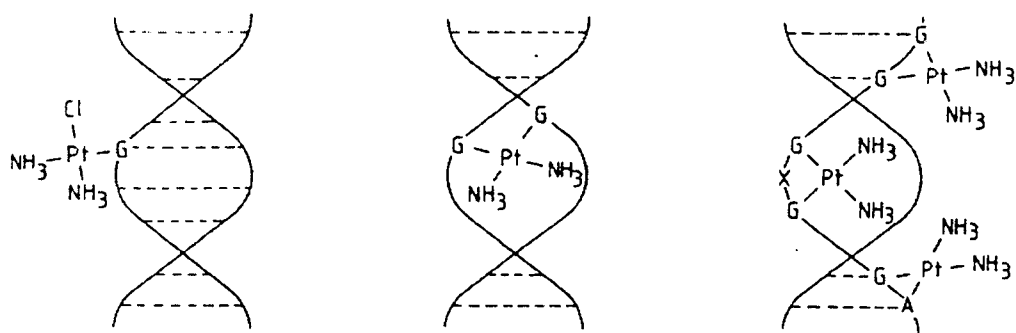
### 1.3.3.2 Interstrand Cross-links

Cisplatin induced interstrand cross-links have been measured both *in vivo* and *in vitro* by alkaline elution techniques. The interstrand cross-links of cisplatin with DNA are now considered to be responsible for cisplatin's cytotoxicity. Initial studies estimated that there are less than 1% to 5% interstrand cross-links among the total Pt-DNA adducts in some mammalian cells, so they were not postulated as the major causes of cisplatin's

anti-tumor activity. Further investigations suggested that interstrand cross-links are important mechanisms of cytotoxicity, since they interfere with DNA synthesis and persist in certain cell lines. The predominant binding sites of cisplatin forming interstrand cross-links to DNA are between two guanine N7 atoms on the opposite strands. Guanine N7 atoms, exposed on the surface of the DNA, are very accessible to metal binding (Sherman et al., 1987). Fram et al. indicate that DNA interstrand cross-links are one of the critical lesions likely to contribute to cytotoxicity by cisplatin. Their study demonstrated up to four fold reduction in DNA interstrand cross-link formation after exposure to cisplatin in resistant BE human colon carcinoma cells compared to its sensitive strain, and loss of resistance was associated with increased interstrand cross-link formation in BE human colon carcinoma cells (Fram et al., 1990).

#### **1.3.3.3 DNA-protein Cross-links**

Besides monoadducts, intrastrand and interstrand cross-links, cisplatin also forms cross-links between DNA and protein. In mammalian cells, cisplatin forms only a small fraction, approximately 0.15%, of its total adducts with protein. Although cisplatin forms cross-links between nuclear DNA and non-histone chromosomal proteins, there is no correlation between the inhibition of DNA synthesis and DNA-protein cross-links. Therefore, the cross-links formed by platinum between DNA and protein are unlikely to be responsible for cisplatin's anti-tumor activity (Sherman et al., 1987).



Monofunctional Adduct

Interstrand Cross-link

Intrastrand Cross-link

Figure 1. 3 Functional binding modes of cisplatin with DNA.

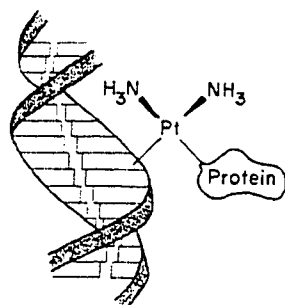


Figure 1. 4. DNA-protein Cross-link

## **1.4 Pharmacology**

The pharmacological characteristics of cisplatin determine its use in the clinical treatment (O'Dwyer et al., 1996). The clinical aspects of cisplatin will be discussed in the following subsections.

### **1.4.1 Clinical Applications**

Cisplatin is administered for clinical use by dissolving its powder formulation with mannitol and 0.9% saline to reach the concentration of 1mg/ml, followed by further dilution in 0.9% NaCl for intravenous administration. Cisplatin prepared in this way is stable for approximately 6 hours (O'Dwyer et al., 1996). In order to minimize cisplatin-induced nephrotoxicity, pre-hydration with one to two liters of salt-containing fluid is usually given to patients (O'Dwyer et al., 1996).

### **1.4.2 Pharmacokinetics**

#### **1.4.2.1 General Parameters**

Following intravenous infusion over 2 to 7 hours, at doses ranging from 50 to 100 mg/m<sup>2</sup>, the plasma cisplatin half-life is approximately 30 minutes (Compendium of

Pharmaceuticals and Specialties, 2001). More than 90% of the cisplatin in the blood plasma is bound to plasma protein at four hours postinfusion (Johnson et al., 2001).

After clinical administration, high concentrations of cisplatin are found in the kidney, liver, intestine, and testes. Lower concentrations are found in the central nervous system, because cisplatin penetrates the blood-brain barrier poorly (Compendium of Pharmaceuticals and Specialties, 2001). Intact cisplatin accounts for the majority of platinum excreted in the urine within 1 hour of administration. Approximately 10 to 40 % of the administered cisplatin is excreted in the urine by 24 hours as various platinum species (Compendium of Pharmaceuticals and Specialties, 2001). Biliary and intestinal excretion of cisplatin appears to be minimal (Goodman and Gilman et al., 1990).

#### **1.4.2.2 Cell Membrane Transport**

The mechanism of cisplatin transport into cells has not yet been conclusively elucidated. It has been suggested that cisplatin uptake is by passive diffusion, since cisplatin accumulation in cells is proportional to the drug concentration. On the other hand, there is evidence supporting the mechanism of active diffusion. Cisplatin uptake in cells can be modulated by a variety of pharmacological agents that do not cause general permeabilisation of the membrane. Other proposed factors that affect intracellular cisplatin accumulation include extracellular pH, osmolality, temperature, and permeability of the plasma membrane (Gately et al., 1993).

### **1.4.3 Mechanism of Action**

#### **1.4.3.1 DNA Interaction**

As previously described, DNA is the major target of cisplatin's anticancer function. Biochemical studies in cultured cells indicated that cisplatin induces different adducts with DNA and further inhibits its synthesis (O'Dwyer et al., 1996).

#### **1.4.3.2 Cisplatin-induced Cell Death**

The sequence of events that leads to cell death after the formation of platinum-DNA adducts have not yet been elucidated. Proliferating cells are more sensitive to cisplatin than non-proliferating cells (Johnson et al., 2001).

The sensitivity of a cell to a platinum drug partially depends on its location in the cell cycle. The study of cisplatin-induced cell death in CHO (Chinese Hamster Ovary) cells indicated that cells experienced slow progression through S phase and accumulated in G<sub>2</sub> phase. At low cisplatin concentration, the cells recovered and continued to progress through the cell cycle. At higher drug concentrations, the cells died, after a protracted G<sub>2</sub> arrest. It was suggested that DNA replication on a damaged template might result in the accumulation of further damage, ultimately causing cell death (Johnson et al., 2001).

Different phenomena regarding cisplatin's relative cytotoxicity to cells in different phases of cell growth were observed by Raaphorst et al.. It was reported that

cisplatin is more cytotoxic in plateau phase than exponential phase for both A2780 cells (human ovarian carcinoma cell line originally derived from an untreated patient (Hamilton et al., 1989)) and 2780<sup>CP</sup> cells (cisplatin-resistant variant obtained by chronic exposure of A2780 to stepwise-increasing concentrations of cisplatin up to 13µg/ml (Lai et al., 1988)). Their opinion is that pH in the medium might affect the cytotoxicity of cisplatin, since the pH of the medium for the cells in exponential phase of 7.1 to 7.3 drops to the range of 6.8 to 6.9 when the cells enter plateau phase (Raaphorst et al., 1996).

In addition to the mounting evidence supporting the existence of programmed death pathways, substantial evidence indicates that cell death is influenced by cellular signal transduction pathways, such as those that control growth, differentiation, and stress response. Some protein kinases are suggested to be involved in transmitting a drug-induced cell death signal (Johnson et al., 2001).

## **1.5 Toxicology**

### **1.5.1 Cisplatin-induced Clinical Side Effects**

The clinical administration of cisplatin is associated with a number of serious side effects, including nausea and vomiting, nephrotoxicity, ototoxicity, neuropathy, and myelosuppression. Rare side effects include visual impairment, seizures, arrhythmias, acute ischemic vascular events, glucose intolerance, and pancreatitis (Johnson et al., 2001).

## **1.5.2 Cisplatin-induced Nephrotoxicity**

The nephrotoxicity of cisplatin almost led to the abandonment of its development for clinical use, until Cvitkovic and colleagues introduced aggressive prehydration, which prevented the development of acute renal failure (Johnson et al., 2001).

### **1.5.2.1 Preclinical Studies**

Cisplatin caused patchy changes in renal proximal convoluted tubules at the cortico-medullary junctions in rats in which it was administered. The tubules were partially lined by flattened epithelial cells lacking brush borders. These cells contained flattened hyperchromatic nuclei. Some appeared enlarged. An occasional mitotic figure was observed. The control rats showed deep cortical proximal tubules lined by regular individual epithelial cells with distinct brush borders (Anand et al., 1993).

Several theories of the mechanism of cisplatin-induced nephrotoxicity have been postulated. In a study of rats treated with cisplatin, a decrease in mitochondrial respiratory function, and an increase in blood urea nitrogen (BUN) and serum creatinine were observed. It has been hypothesized that cisplatin-induced nephrotoxicity is related to its affinity to the sulfhydryl group of various enzymes (Anand et al., 1993) (Kuhlmann et al., 1997).

Another theory explaining cisplatin-induced nephrotoxicity is that cisplatin interferes with the mechanism that controls cellular homeostasis. In a study of rat kidney

cells, cisplatin administration was associated with increased renal endoplasmic reticulum calcium pump activity. This activity occurred within four hours and preceded an increase in BUN and serum creatinine by at least one day. It was suggested the change of endoplasmic reticulum calcium pump activity might be a useful biomarker for cellular toxicity and a factor of the mechanism of this toxicity. But detection of this response requires analysis of tissue sections and would not be used in the clinical detection of nephrotoxicity (Anand et al., 1993).

Lee K. Tay et al observed that cisplatin inhibited DNA synthesis to a greater extent than RNA and protein synthesis in both rabbit kidneys *in vivo*, and rabbit renal proximal tubule cells, *in vitro*. They suggested that inhibition of renal intracellular synthetic activity by cisplatin, rather than its effect on enzyme activity, precedes the onset of cell lethality and may be an important event in the initiation of cisplatin-induced nephrotoxicity (Tay et al., 1988). Robert et al. have suggested that total DNA adducts can be linked to cisplatin's antitumor response; they also proposed that the mechanism of cisplatin-induced nephrotoxicity might be associated with cisplatin's ability to bind with DNA (Robert et al., 1986).

### **1.5.2.2 Clinical Studies**

Nephrotoxicity is ameliorated but not completely prevented by hydration (Johnson et al., 2001). In humans, renal damage has been observed at cisplatin doses of 50 mg/m<sup>2</sup> given without adequate hydration (Pinzani et al., 1994). In one study of the

effect of cisplatin on renal structure in human, tubular necrosis was observed in the proximal and distal tubules at three weeks after the last course of cisplatin administration (Dentino et al., 1978). It has been suggested that proximal, as well as distal, portions of renal tubules are injured to some extent by cisplatin administration (Anand et al., 1993).

Cisplatin-induced nephrotoxicity is the principle dose-limiting factor in clinical administration (Nagai, et al., 1996). Acute tubular necrosis has been observed in the human kidney, followed by chronic pathological damage persisting for more than twelve months (Dentino, et al., 1978, Gonzalez-Vitale et al., 1977). The urinary excretions of  $\beta_2$ -microglobulin, alanine aminopeptidase, and N-acetyl- $\beta$ -glucosaminidase have been used as markers for acute kidney lesions (Buamah et al., 1982). A decrease in glomerular filtration rate (GFR), and increases in serum creatinine (SCr), and blood urea nitrogen (BUN) after cisplatin administration for a week to several months, suggest that cisplatin may cause further damage in both the glomerulus and distal tubules (Meijer et al., 1983) (Fjeldborg et al., 1986) (Nagai, et al., 1996). Hypomagnesemia, hypocalcemia and hypokalemia have also been observed after cisplatin administration (Daugaard et al., 1988) (Buckley et al., 1984) (Nagai, et al., 1996).

According to the study by Stewart et al (1985) of autopsy kidney-cortex platinum concentrations from patients who received cisplatin 0-240 days antemortem, cisplatin nephrotoxicity was correlated with kidney-cortex platinum concentrations (Stewart et al., 1985). In the more recent analysis by Stewart et al (1994), they showed that the cisplatin dose per course was more closely associated with kidney-cortex platinum concentrations than the cumulative cisplatin doses. One explanation for the above results was that most of the drug is washed out of the kidney after each treatment,

and the more recent or the last treatment course (before death) accounts for most of the drug retention in the kidney; the other explanation was that patients who experienced early nephrotoxicity therefore might have had future treatment limited. (Stewart et al., 1994)

### **1.6 The Strength and Weakness of Current Knowledge**

The mechanism of cisplatin-induced cytotoxicity in cancer cells has been extensively studied, as previously described. The mechanisms of cisplatin-induced nephrotoxicity have been less extensively studied and are less well known (Pinzani et al., 1994).

*In vitro*, the LLC-PK<sub>1</sub> cell line (derived from porcine kidney proximal tubule cells) has been used to investigate cisplatin-induced nephrotoxicity. DNA synthesis in LLC-PK<sub>1</sub> cells is sensitive to cisplatin exposure. After exposure to 200  $\mu$ M cisplatin for one hour, DNA synthesis was reduced 76% compared with the control (Montine et al., 1988). Distal tubular cells have been less extensively used as *in vitro* models of clinical cisplatin-induced nephrotoxicity than proximal tubular cells. Delbancut et al. have used both the MDCK (derived from canine kidney distal tubule cells) and LLC-PK<sub>1</sub> cell lines as *in vitro* models to evaluate the cisplatin-induced cytotoxicity in distal and proximal tubules of the kidney. Their results demonstrated that cisplatin induced cytotoxicity at both the distal and proximal tubule cells (Delbancut et al., 1994). However, they did not present data on the mechanism of cisplatin cytotoxicity in these two cell lines.

*In vivo*, the mechanism of cisplatin-induced nephrotoxicity in proximal segments of the renal nephron has been evaluated. Field et al. suggested that cisplatin reduces proximal tubule sodium reabsorption by inhibiting the entry of sodium into the cells across the apical membrane in rat kidney. Cisplatin inhibits the entry of sodium into proximal cells possibly by interfering with the function of the Na-H exchanger in the apical membrane. Electrophysiological data in a micropuncture study by Allen and Barratt were consistent with enhanced sodium transport by late distal segments after cisplatin infusion in the rat. Conclusive data to explain cisplatin's effects on transport in distal nephron segments has not been published (Field et al., 1989).

Cisplatin is taken up by renal tubular cells, reaching its highest concentrations in the renal tubular cells of the inner cortex and outer medulla, which include cells of the proximal tubule and thick ascending limb of Henle (Blachely et al., 1981). Cisplatin administration causes impairment of proximal tubular re-absorption, but distal tubular function also seems to be affected (Pinzani et al., 1994). Kröning et al. postulated that mouse proximal tubule cells were more sensitive to cisplatin toxic effects than distal tubule cells, and that this difference was due to decreased platinum uptake in proximal tubule cells compared to distal tubule cells (Kröning et al., 1999).

As an anticancer chemotherapeutic drug, cisplatin is used for treatment of a variety of cancers. Nephrotoxicity has been one of the severe side effects limiting the use of this drug. To my knowledge, a definitive explanation of cisplatin-induced nephrotoxicity has not been elucidated. Understanding the mechanism of cisplatin-induced cytotoxicity in distal renal tubular cells *in vitro*, may ultimately lead to strategies to ameliorate clinical human nephrotoxicity. With the development of successful

approaches for reducing cisplatin's renal toxicity, one may be able to increase cisplatin's therapeutic index, in future.

## **1.7 Hypothesis and Specific Aims for This Project**

### **1.7.1 Hypothesis**

A mechanism of cisplatin-induced cytotoxicity in MDCK cells relates to its ability to bind to DNA and interfere with its synthesis.

### **1.7.2 Specific Aims of This Project**

1. Use MDCK cells as an *in vitro* model of cisplatin-induced nephrotoxicity.
2. Determine the cytotoxicity of cisplatin to MDCK cells.
3. Correlate this cytotoxicity with cisplatin's effects on DNA in MDCK cells.

## 2. Materials and Methodology

### 2.1 Cell Line

The *in vitro* model allows good quantitative characterization of cisplatin uptake and the timing of exposure, and accurate measurement of cisplatin accumulation in cultured cells (Kröning et al., 1999). The ideal cell line as an *in vitro* model of human nephrotoxicity would be a normal human kidney cell line. Human kidney cells, which can be obtained from normal human organ donors, can only undergo a maximum of three passages (Clonetics, San Diego, CA, USA). The finite lifespan of these normal cells makes it difficult for it to be a good model *in vitro*. Another human renal cell line (the 786-O von Hippel-Lindau tumor suppressor gene positive cell line) was derived from transformed primary human renal cancer cells. The von Hippel-Lindau gene has been implicated as the first tumor suppressor gene involved in the regulation of cell cycle exit, which is consistent with its gatekeeper function in the kidney; but it is still controversial whether the 786-O (von Hippel-Lindau tumor suppressor positive) cell line is a normal kidney cell line (Pause et al., 1998). Immortalized animal kidney cells, such as MDCK cells, are probably the models that are the closest to normal human kidney cells, and hence are probably the models preferred for studies of cisplatin nephrotoxicity.

MDCK (Madin-Darby canine kidney) cells, which were purchased from ATCC (American Type Culture Collection, Rockville, MD, USA), are kidney epithelial distal tubular cells initially derived from a normal female cocker spaniel. The cells were derived by S. H. Madin et al. in 1958. The cells were immortalized by partial

trypsinization with trypsin-versene solution. This resulted in serial passages without difficulty. At 49 passages, the cells were donated to ATCC.

Cells of the MDCK line have a distinctive epithelioid morphology. MDCK cells display several functional and anatomical properties of normal kidney tubular cells; such as possessing brush borders, forming tight junctions, and catalyzing unidirectional sodium transport. MDCK cells can grow in serum free medium with purified hormones and serum factors. Although this cell line forms small colonies, which is important for clonogenic assay, and proliferates at the top of mouse monolayer cultures, it does not form tumors in adult nude mice. Previous studies indicated that MDCK cells retain normal kidney-specific properties, regional differentiation of the cell surface membranes, and potential for the regeneration of functional kidney tubules (Saier et al., 1982).

## **2.2 Methodology to be Used for This Project**

MDCK cells are exposed to MEM (Minimal Essential Medium Alpha Medium) containing cisplatin at various concentrations for one hour. There are two reasons for choosing a one hour exposure: 1) According to Mistry et al., cisplatin's concentrations in the kidney cortex and medulla reached its maximal level within one hour of the i.p. injection of 5 mg/kg cisplatin in rats (Mistry et al.,1989). 2) Cisplatin's half-life is about 30 minutes after i.v. administration in humans (Compendium of Pharmaceuticals and Specialties, 2001).

## **2.3 Growth Curve of MDCK Cells**

### **2.3.1 Materials**

#### Chemicals:

MEM Alpha Medium (Minimum Essential Medium Alpha Medium), 10X PBS (phosphate buffered saline, pH 7.4), FBS (fetal bovine serum), and 0.25% trypsin-EDTA were purchased from Gibco BRL Life Technologies (Grand Island, NY, USA). Trypan blue was purchased from Sigma Chemical Co. (St. Louis, MO, USA).

#### Cell Line:

The non-malignant dog kidney epithelial distal tubule cells (MDCK) were purchased from ATCC. The cells were grown on T-25 tissue culture flasks in an incubator at 37°C with a humidified atmosphere of 5% CO<sub>2</sub> and 95% air. The cells were maintained in MEM medium with 10% of heat-inactivated fetal bovine serum without any antibiotics.

#### Equipment:

Cells were examined with a microscope (model: CK2), which was manufactured by Olympus (Japan); hemocytometer (Model: 235,962-9) was from Sigma Chemical Co. (St. Louis, MO, USA).

### 2. 3. 2 Methods

The growth characteristics of the MDCK cell line were studied in order to establish the standard growth condition for the experiments. Experiments were set up in three groups; each of them included 99 T-25 flasks (Becton Dickson, NJ, USA). On day zero, each group of T-25 flasks were seeded with  $5 \times 10^5$  cells,  $1 \times 10^6$  cells, and  $1.5 \times 10^6$  cells respectively, and the cells were incubated as previously described. On the following eleven days, three flasks were taken out of the incubator from each group at a period of every twenty-four hours. The cells were washed twice in 5 ml PBS, and this was followed by an addition of 500  $\mu$ l 0.25% trypsin EDTA for 20 minutes. After the cells were harvested and diluted in MEM medium with 10% FBS, they were stained with trypan blue and counted with a hemocytometer slide under a microscope.

The total cell numbers were determined by counting each group of cells in triplicate and averaging the numbers each day. One and one-half million cells were seeded in the flasks at day zero, and those cells reached plateau phase at day four. The group of flasks, which were seeded with  $1.5 \times 10^6$  cells at day zero, was selected for the rest of the experiments, since they reached the plateau phase in a relatively shorter period. These experiments were conducted in triplicate.

## **2. 4 Cisplatin-induced Cytotoxicity**

### **2. 4. 1 Materials**

#### Chemicals and Reagents:

Clinical formulation of cisplatin (1mg / ml or 3.33 mM, pH 7.3) in 0.9% saline was purchased from Faulding Canada Inc. (Vaudreuil, QC, Canada). Saline was obtained from Baxter Corporation (Toronto, ON, Canada). All experiments required lower drug concentrations, which were achieved by dilution of the clinical solution with 0.9% saline. MEM, PBS, and 0.25% trypsin-EDTA were purchased as described in 2.3.1. Methylene blue was purchased from Sigma (St Louis, MO, USA). Five cm petri dishes and 10 cm petri dishes were purchased from Becton Dickson and Co. (NJ, USA).

### **2. 4. 2 Methods**

One and one-half million cells were seeded in 5 cm petri dishes on day zero. After growing for three days, the cells were washed twice in PBS, and then exposed to medium without fetal bovine serum and cisplatin at various concentrations for one hour at 37 °C. Cisplatin was diluted in fresh 0.9% saline, and then added to 5 ml of medium immediately to reach exposure concentrations ranging from 0  $\mu$ M to 100  $\mu$ M. After the one-hour exposure, the drug-containing medium was aspirated, and the cells were rinsed in PBS three times. After trypsinization, the cells were harvested and diluted in MEM

with 10% FBS, and counted by the method described in section 2.3.2. Cells were reseeded in 10 cm petri dishes in triplicate at the density of 1000 cells per dish for the control and 5000 cells per dish for the drug treated samples.

After 10 days of incubation, the medium was aspirated, and the cells were fixed and stained with methylene blue. Cultures of cells containing at least 50 cells were counted as one colony under a microscope. It was assumed that each colony originated from a single surviving cell, which had attached to the growing surface and continued to divide. Clonogenic assays were performed in quadruplicate. Considering the average number of colonies in control dish as 100%, the percentage of colonies in each dish was calculated; the average and standard deviation of percentage of colonies for each concentration were calculated.

## **2.5 Cellular Accumulation of Platinum:**

### **2.5.1 Atomic Absorption Spectrophotometry:**

The atom is made up of a nucleus surrounded by electrons. Every element has a unique number of electrons, which are associated with the atomic nucleus in an orbital structure, which are different for each element (Beatty, 1988).

The ground state is the most stable electronic configuration of an atom. When light of an appropriate wavelength hits an atom in its “ground state”, the atom can absorb light and turn into a less stable configuration state, the “excited state”. From the unstable

“excited state”, the atom will spontaneously return to its ground state. A displaced electron will quickly return to its previous orbital position, and radiant energy, the same as the energy of the absorbed light, will be emitted. This property of atoms to absorb light of a particular wavelength is utilized in an atomic absorption spectrophotometer (Gaffin, 1979).

This method measures the amount of light of a specific wavelength absorbed by an atom cloud. Supplying enough thermal energy to the sample to dissociate the chemical compounds into free atoms produces the atom cloud required for atomic absorption measurements. The absorbance shows a linear relationship with concentration. Beer’s law defines this relationship:  $A=abc$ , where “A” is absorbance, “a” is the absorption coefficient that is characteristic for the absorbing species, “b” is the length of the light path, and “c” is the concentration of the absorbing substance (Gaffin, 1979).

Atomic absorption spectrophotometry has been evolving since 1960. The atomic absorption apparatus requires a light source, a sample cell and detector. Since the atom absorbs light at a particular wavelength, it is very important to use a light source, which emits a specific wavelength that can be absorbed by the atom of interest. Narrow line sources make this technique not only sensitive but also very specific. The most common source, the “hollow cathode lamp”, was installed in the instrument used in this study (Gaffin, 1979).

With flameless atomic absorption spectroscopy, a graphic furnace is used as a flameless sampling device. In this technique, a tube of graphite is located in the sample compartment of the atomic absorption spectrometer, with the light path passing through

it. A small volume of sample solution is placed into the tube. The tube is heated through a programmed temperature sequence for drying, ashing and atomization (Beatty, 1988).

As the atoms are generated and diffused out of the tube, the absorbance rises and falls in a peak-shaped signal. The peak height and integrated peak area are used as the analytical signal for quantitation. (Beatty, 1988)

Atomic absorption detection limit for platinum element is about 50 ng/ml for furnace graphite atomic absorption spectroscopy with the instrument used for this study. Table 2.1 represents a diagram of the temperature program for the determination of platinum in a cell suspension sample.

As it is shown in Table 2.1, eleven different steps are presented in this program. Steps one to three involve drying, steps four and five involve ashing with a temperature of 1200°C, step six involves the preparation for atomization. Steps seven to nine involve atomization at temperatures of 2700 °C. Steps ten to eleven are for cleaning and re-setup purposes.

Step	Temperature (°C)	Time (S)
1	80	15
2	100	10
3	100	35
4	1200	25
5	1200	20
6	1500	10
7	2700	1.0
8	2700	2.0
9	2700	1.0
10	40	12
11	40	3.0

**Table 2.1:** Furnace operating parameter for the measurements of Pt in a cell suspension sample

Element	Lamp current at mA	Wavelength nm	Maximum Ash°C	Atomize °C
Pt	10	265.9	1200	2700

**Table 2.2** Parameters of Pt assay by atomic absorption spectrophotometry

## 2.5.2 Materials

### Cell line, Medium, and Drug:

Cell line, medium and cisplatin have been described in section 2.3.1.

### Equipment:

V. Plateau tubes were supplied by Seigniory Chemical Products Ltd. (St-Laurent, QC, Canada). The atomic spectrophotometer (model AA-1475) and graphite tube atomizer (model GTA-95) were supplied by Varian Canada Inc. (Ottawa, ON, Canada). The spectrophotometer was operated at an excitation wavelength of 265.9 nm. A hollow cathode lamp (L233) made by Hamamatsu photonics K.K. (Japan) was used for the source of narrow light, and the current was adjusted to 10 mA. A polytron homogenizer, model V.C. 375, was supplied by Sonic & Materials Inc. (Danbury, CT, USA), and was used with a 90% output at 5 pulses per second. A coulter cell counter (model ZM) was supplied by Coulter Electronic Ltd. (England).

## 2.5.3 Methods

MDCK cells were plated in triplicate in 5 cm petri dishes at the density of  $1.5 \times 10^6$  per dish for three days, and then exposed to cisplatin at concentrations of 50  $\mu\text{M}$  to 100  $\mu\text{M}$  for one hour in the incubator as described before. The exposure concentrations were selected to account for the detection limit of platinum at 50 ng/ml by the atomic

absorption spectrometer (A.A.). After aspiration of the medium, the dishes were washed rapidly by immersing them in three beakers containing 1 liter of ice cold PBS. Five hundred  $\mu\text{l}$  of trypsin-EDTA was added to each dish, and the cells were incubated for 20 minutes at 37 °C. Cell suspensions were suspended by a pipette to lift the cells completely off the tissue culture dishes. The resulting cell suspensions from each tissue culture dish were collected in separate tubes. Cell suspensions were re-suspended by vortexing, and 100  $\mu\text{l}$  from each tube was used to count the cells. Four hundred  $\mu\text{l}$  EME with 10% FBS was added to the tube containing the cells to be counted, in order to inhibit the further digestion by trypsin-EDTA. Four hundred  $\mu\text{l}$  of each cell suspension was taken from the diluted suspension after vortexing for counting. The counting was conducted in quadruplicate. The remainder of each cell suspension was collected for the measurement of the cellular platinum content.

A standard curve of platinum measurement by atomic absorption spectrophotometer was obtained by injecting into the flameless atomic absorption spectrophotometer 30  $\mu\text{l}$  of a clinical formulation of cisplatin at concentrations of 50 ng/ml, 100 ng/ml, 250 ng/ml, and 500 ng/ml. Temperature programming of the atomic absorption spectrophotometer was described in table 2.1. Cell suspensions were sonicated by a Polytron homogenizer for 35 seconds and then repeated four more times until a homogeneous suspension was obtained. Each suspension was vigorously vortexed for 30 seconds, and then 30  $\mu\text{l}$  of the uniform suspension was injected directly into the graphite plateau tube by using an appropriately sized pipette. The injection of each concentration of the standard curve and of each sample was conducted for a minimum of three times, and the experiments were repeated in triplicate.

Intracellular platinum accumulation of the cells in different tissue culture dishes were calculated in ng of platinum per million cells, by using the concentration of platinum measured by atomic absorption spectroscopy and the numbers of cells counted by the cell counter.

## **2.6 Platinum Binding with DNA:**

### **2.6.1 Materials**

#### Cell line, Medium, and Drug:

Cell line, medium, and cisplatin used for this experiment have been described in 2.3.1.

#### DNA Isolation Reagents:

A Wizard Genomic DNA purification kit was purchased from Promega Corporation (Madison, WI, USA). The Wizard Genomic DNA purification kit contained nuclei lysis solution, RNase solution, protein precipitation solution, and DNA rehydration solution. Room temperature isopropanol and 70% ethanol were used for isolating and washing DNA.

### Equipment:

U.V. Visible Spectrophotometer (Model: Cary), which was made by Varian Australia PTY Ltd., was used for measuring the quantity of isolated DNA. Micro-centrifuge (Model: Micromax) was manufactured by IEC International Equipment Company (MA, USA)

### **2.6.2 Methods**

DNA isolation was done according to the method from Promega (Promega Corporation, Madison, WI, USA). Four million cells were seeded in the 10 cm petri dishes for three days, and then the cells were exposed to cisplatin at concentrations from 1.5 mM to 3 mM, in the incubator for one hour. Exposure concentrations were selected according to the detection limitation of the A.A. as described previously and the limitation of cisplatin's solubility in saline, which is 3.3 mM. After aspiration of the medium, the dishes were washed rapidly by immersing them in three beakers containing 1 liter of ice cold PBS. One ml of trypsin-EDTA was added to each dish, and the cells were incubated for 20 minutes at 37 °C. Each cell suspension was suspended by a pipette to lift the cells completely off the tissue culture dishes. The resulting cell suspensions from each tissue culture dish were collected in separate tubes.

After the cells were harvested with trypsin, they were transferred to a 1.5 ml micro-centrifuge tube. Cells were centrifuged at 16,000 x g for 10 seconds to form a pellet. The supernatant was removed, leaving behind the cell pellet plus 10-50 µl of

residual liquid. Two hundred  $\mu\text{l}$  of PBS was added to wash the cells, and they were then centrifuged at 16,000 x g for 10 seconds to re-pellet the cells. PBS was removed from the micro-centrifuge tube, and the tube was vortexed vigorously to re-suspend the cells.

After adding 600  $\mu\text{l}$  of nuclei lysis solution to the cells, each cell suspension was pipetted to lyse the cells, until the visible cell clumps disappeared. Then, 3  $\mu\text{l}$  of RNase solution was added to the nuclear lysate, and the samples were mixed by inverting twenty five times. The mixtures were incubated at 37°C for 30 minutes.

After the samples were cooled for five minutes to room temperature, 200  $\mu\text{l}$  of protein precipitation solution was added to each sample and the mixtures were vortexed vigorously at high speed for 20 seconds. The samples were chilled on ice for 5 minutes, and then centrifuged at 16,000 x g by a micro-centrifuge for 4 minutes. The precipitated protein formed a tight white pellet. The supernatant containing DNA was carefully removed into a clean 1.5 ml eppendorf tube (leaving the protein pellet behind), which contained 600  $\mu\text{l}$  of room temperature isopropanol. A small quantity of supernatant, which might have contained protein, was left behind in the original tube to avoid contaminating the DNA solution with protein.

The solution, containing DNA and isopropanol, was gently mixed by inversion until the white thread-like strands of DNA formed a visible mass. The solution was centrifuged for 1 minute at 16, 000 x g at room temperature, then the DNA formed a small white pellet on the bottom of the centrifuge tube. The isopropanol was carefully decanted, and the DNA was washed by adding 600  $\mu\text{l}$  of room temperature 70% ethanol. The tubes containing samples were gently inverted several times to wash the DNA.

The micro-centrifuge tubes containing DNA were re-centrifuged at 16, 000 x g for 1 minute at room temperature. The ethanol was carefully aspirated by using a pipette. The DNA pellets were very loose at this point; therefore, they had to be handled carefully to avoid being aspirated into the pipette. The tubes were inverted on clean absorbent paper and the pellets were air dried for 15 minutes.

DNA was dissolved in 110 µl of DNA dehydration solution overnight at room temperature. The quantity and purity of the DNA was measured by an U.V. Visible Spectrophotometer (Varian). The readings for quantitating the amount of DNA were taken at wavelengths of 260 nm and 280 nm according to the method of Irwin et al. (Irwin et al., 1989).

The quantity of platinum accumulated in DNA was detected by atomic absorption spectrophotometry, and the samples were measured by the same method as previously described in section 2. 5. 3.

## **2.7 Cisplatin-induced DNA Synthesis Inhibition:**

### **2.7.1 Background**

5-Bromo-2'-deoxy-uridine (BrdU), a brominated analog of thymidine, can be incorporated specifically into DNA in place of thymidine (Sigma, St. Louis, MO). Cells, which are synthesizing DNA in S phase of the cell cycle, can be labeled with BrdU. A monoclonal antibody directed against BrdU and a fluorochrome-conjugated secondary

antibody can be used to quickly identify those cells, which are undergoing DNA synthesis during exposure to BrdU (Boehringer Mannheim, Germany). The proportion of cells in S phase can be determined by fluorescence microscopy or by flow cytometric analysis (Becton Dickinson Immunocytometry Systems, Mountain View, CA, USA). The fluorescence intensity per cell is directly proportional to the amount of BrdU incorporated and therefore provides a rapid method for detecting the rate of cellular DNA synthesis (Gratzner, 1982).

For this assay, cells are incubated *in vitro* with 10  $\mu$ M BrdU for approximately 30 minutes. The samples are fixed with ethanol and incubated with an anti BrdU monoclonal antibody. The monoclonal antibody binds to BrdU incorporated with DNA. Normally binding of the antibody is only achieved by denaturation of the DNA. This is usually obtained by exposing the cells to acid, base or heat. However, these procedures result in the destruction of cell integrity. The BrdU Labeling and Detection Kit I used in our experiments avoids these problems. The antibody preparation contains specific nucleases, which allow the antibody to bind BrdU after fixation in acidic ethanol. After incubation with anti-mouse-Ig-fluorescein, bound anti-BrdU monoclonal antibody is visualized by immunofluorescence microscopy (Boehringer Mannheim, Germany).

## 2.7.2 Materials

### Cell Line, Medium, and Drug:

Cell line, medium, and cisplatin have been described in 2.3.1.

### Reagents:

BrdU Labeling and Detection Kit I was purchased from Boehringer Mannheim (Germany). Hoechst stain was purchased from Sigma-Aldrich Canada Ltd. (St Louis, MO, USA). The BrdU labeling and detection kit I contained BrdU labeling reagent (1000 x conc.) in 10 mM sterile phosphate buffered saline; 100 ml PBS (10 x conc.); incubation buffer containing 66 mM tris-buffer, 0.66 mM MgCl<sub>2</sub>, 1 mM 2-mercaptoethanol; anti-BrdU, mouse monoclonal antibody containing nucleases for DNA denaturation in PBS and glycerine; immunosorptively purified and stabilized anti-mouse-Ig-fluorescein. Mounting medium for fluorescence microscopy was purchased from Kirkegaard & Perry Laboratories (Gaithersburg, Maryland, USA).

### Equipment:

Fluorescence microscope (Model: BX-50) was manufactured by Olympus. The Image-Pro-Plus software for fluorescence microscope image analysis was supplied by Media Cybernetics (Maryland, USA)

### 2.7.3 Methods

The DNA synthesis assay was conducted according to the modified protocol of immunofluorescence assay for the detection of BrdU incorporated into cellular DNA offered by Boehringer Mannheim. Two 1.5 cm OD sterile cover slips were placed in each well of two multiwell (6 wells) dishes (Becton Dickinson, NJ, USA). Four hundred thousand cells were seeded in each well. After the cells grew on the top of the cover slips for three days, the medium was aspirated and the cells were washed in 2 ml of PBS three times. MEM without FBS was added to the cells, and they were exposed to cisplatin at concentrations ranging from 0  $\mu\text{M}$  to 100  $\mu\text{M}$  for one hour in an incubator with conditions as previously described. The range of exposure concentrations was the same as that used in the clonogenic assay assessing cisplatin-induced cytotoxicity in MDCK cells. The cells were taken out of the incubator, and the medium was aspirated. Two ml of PBS was added to the cells in order to wash the cisplatin away. To each well of cells, 2 ml of culture medium was added, and followed by BrdU labeling reagent. Two  $\mu\text{l}$  of BrdU was added directly to the culture medium to achieve a final concentration of 10  $\mu\text{M}$ . After the cells were incubated for 2 hours in 5%  $\text{CO}_2$  at 37  $^\circ\text{C}$ , the BrdU and medium were aspirated. The cover slips were taken out and washed in PBS four times; then the cells were fixed in 70% ethanol (in 50mM glycine buffer, pH 2) for about 45 minutes at -20  $^\circ\text{C}$ . The cover slips were washed in washing buffer four times. The anti-BrdU solution was diluted with incubation buffer at 1:10 shortly before use. Then the cells were incubated with the diluted anti-BrdU solution for 30 minutes at 37  $^\circ\text{C}$ . The cover slips were washed four times in washing buffer, then incubated with anti-mouse-Ig-fluorescein (FITC) for 30 minutes at 37  $^\circ\text{C}$ , and then the cover slips were washed with

PBS three times. The cells were incubated for 1 minute with 5  $\mu$ M of Hoechst stain. The nuclei were stained by Hoechst, which was visualized by excitation at 352 nm and emission at 461nm. The excitation and emission maximum for FITC (fluorescein isothiocyanate) is 492 nm and 520 nm, respectively. The cells on cover slips were washed with PBS, dried and Flo-Texx Mounting Medium was applied prior to microscopic examination (Olympus BX-50).

## **2.8 Cisplatin-induced Pt-DNA Interstrand Cross-links**

### **2.8.1 Background**

The comet assay, which is also called single cell gel assay (SCG), single cell gel electrophoresis (SCGE) or microgel electrophoresis (MGE), was first introduced by Östling and Johanson in 1984 as a micro-electrophoretic technique for the direct visualization of DNA damage in individual cells. In the original version of the assay, small quantities of cells are suspended in a thin agarose gel on a microscope slide. Cells are lysed, electrophoresed, and stained with a fluorescent DNA affinity dye. The electric current pulls the negatively charged DNA fragments, allowing the relaxed and broken DNA from the nucleus to migrate further towards the anode. The resulting images, which are named “comets” because of their appearance, are visualized by a fluorescent microscope and are analyzed to determine the extent of DNA damage. Östling and Johanson observed that the amount of DNA released from the head of the comet during electrophoresis is proportional with the dose of radiation. Subsequently, similar

observations in other laboratories indicated that this assay might allow for the prediction of tumor responses to radio- and chemotherapy regimens (Fairbairn et al., 1995).

The comet assay is a particularly valuable technique, which allows for the detection of DNA damage in virtually any eukaryote cell population that can be prepared in single cell suspension. It requires as few as one thousand cells, and the results can be obtained in one to two days. Except for the image analysis, a great advantage of the comet assay is the extremely low cost of performing the assay. Schmezer and colleagues have compared the sensitivity of the comet assay to other methods, which measure average DNA damage in a population of cells. It was found that the sensitivity of SCGE assay is similar to the alkaline elution assay (McKelvey et al., 1993).

Due to the neutral pH lysis conditions used by the neutral version of the comet assay, only DNA double-strand breaks can be detected. Procedures for measuring DNA strand breaks are based on the principle that strand-breaking agents reduce the size of the large duplex DNA molecules. Because of DNA supercoiling and tight packaging within the nucleus, assays that measure DNA single strand breaks generally require unwinding of the double strand DNA molecule for sensitive detection. The loss of DNA supercoiling creates a sensitive assay for the presence of single-strand breaks. A pH higher than 12.3 is used to facilitate denaturation, unwinding, and expression of single strand breaks. Therefore, single DNA strand breaks become apparent only after exposure to alkaline conditions. Ten years ago, the alkaline comet assay was developed by modifying the denaturing conditions of the neutral comet assay in this way in order to measure DNA single strand breaks (Fairbairn et al., 1995).

The MGE method has been progressively improved for sensitivity and reproducibility for the detection of single strand breaks. Alkaline conditions cause denaturation of duplex DNA, and allows the individual strands to separate and migrate independently (Olive, 1999). Rydberg and Johanson first described an assay detecting DNA single-strand breaks in individual cells. In this assay, cells are embedded in agarose on a microscope slide and lysed under mildly alkaline conditions in order to allow a partial unwinding of DNA. The slides are neutralized and stained for analysis by using acridine orange (Fairbairn et al., 1995).

Comets form when broken ends of the negatively charged DNA molecules become free to migrate in the electric field towards the anode. The ability of DNA to migrate is a function of both the size of the DNA and the number of broken “ends”, which may be attached to large pieces of DNA but still migrate a short distance from the comet head. Tail length initially increases with damage but reaches a maximum that is largely defined by the electrophoresis conditions, not the size of the fragments. At low damage levels, stretching of attached strands of DNA, rather than migration of individual pieces, is likely to occur. With the increasing number of breaks, DNA pieces migrate freely into the tail of the comet, and at the maximum level (e.g. apoptotic cells); the head and tail are well separated. The intensity of the fluorescence in the tail relative to the head provides information about the numbers of strand breaks. These two concepts, stretching and migration of separated strands, are generally accepted to explain the DNA migration patterns observed in the comet assay (Fairbairn et al., 1995).

An increasingly popular method of comet analysis is an endpoint referred to as the “tail moment”, which is defined as the product of the distance between the center of

mass of the head and the center of mass of the tail, and the fraction of total DNA found in the tail (Olive et al., 1990). Tail moment incorporates a measure of both the smallest detectable size of migrating DNA and the number of relaxed or broken DNA pieces. (Fairbairn et al., 1995).

The comet assay has been widely used in radiation biology to measure excisable DNA damage, DNA cross-links, apoptosis, and oxidative damage. Genomic interstrand cross-link formation in cells has been measured most frequently using the alkaline elution technique (Fairbairn et al., 1995).

Interstrand cross-links induced by nitrogen mustard and cisplatin have been measured by the comet assay. The principle of the experiment is that increasing numbers of cross-links prevent the migration of DNA damaged by X-rays. It is conceivable that a standardized strand break induction system can be used to determine the ability of different agents to cause DNA migration inhibition by interstrand cross-link formation (Fairbairn et al., 1995).

McNamee and colleagues modified the original alkaline comet assay based on the method of Singh and colleagues. The modified protocol increases productivity and efficiency without sacrificing assay reliability. In the original protocol, a small number of cells are sandwiched between thin layers of agarose on a glass microscope slide. Usually, only one or two samples can be cast on each glass slide, which must be handled separately for each of the lysis, electrophoresis and staining steps. In this modified protocol, up to eight samples can be cast in individual wells of super cell chambers affixed to one gel bond film. The modified protocol provides the facility of processing numerous samples with minimal effort (McNamee et al., 2000).

The agarose gel bond films are stable when dry and suitable for analysis or independent verification of results. The SYBR gold stain possesses ideal properties for automated scoring of comets due to its intense staining and greater resistance to fading compared with propidium iodide (McNamee et al., 2000).

Since platinum binding to DNA in the toxicity range could not be detected by atomic absorption, platinum-DNA interstrand cross-links were measured by the version of the alkaline comet assay developed by McNamee and colleagues.

## **2.8.2 Materials**

### Cell line, Medium, and Drug:

The same cell line, culture medium and cisplatin were used as described in 2.3.1.

### Chemical Reagents for the Comet Assay:

A solution of 0.75% w/v low melting DNA grade agarose (NJ, USA, Fisher Biotech) was freshly prepared in PBS containing 58 mM Na<sub>2</sub>HPO<sub>4</sub>, 17 mM KH<sub>2</sub>PO<sub>4</sub>, 68 mM NaCl, pH 7.4 (Gibco BRL, Grand Island, NY, USA).

Aqueous solutions, dilutions and rinses were all made with double distilled water. Lysis buffer A (pH 10.0) consisting of 2.5 M NaCl, 100 mM Tetrasodium EDTA, 10 mM Tris base, and 1% N-lauryl-sarcosine (w/v) was supplemented with 1% Triton X-100 and 10 % DMSO (v/v) (Sigma-Aldrich, St. Louis, MO, USA) immediately before use.

Lysis buffer B (pH 10.0) contained of 2.5 M NaCl, 100 mM Tetrasodium EDTA, and 10 mM Tris base. Proteinase K (Sigma-Aldrich, St. Louis, MO, USA) was prepared in a solution of 20 mg/ml in TE buffer (Promega, Madison, WI, USA) and stored in 2 ml aliquots at -30 °C. Proteinase K at 1 mg/ml was added to lysis buffer B immediately before use. Both lysis buffer A and lysis buffer B were stored at room temperature in the dark.

The electrophoresis buffer (pH 13.1) consisting of 0.3 M NaOH, 10 mM tetrasodium EDTA (Pittsburgh, PA, USA, Fisher Scientific), 0.1% (w/v) 8-hydroxyquinoline (Sigma-Aldrich, St. Louis, MO, USA), and 2% (v/v) DMSO (Fisher Scientific, NJ, USA) was made freshly on the same day of the experiment. A 1 M ammonium acetate solution was prepared in water and stored at room temperature. SYRB Gold stain (Molecular Probes, Eugene, OR, USA), was prepared in water and stored at the temperature of 4 °C in the dark before fluorescence microscopy analysis.

#### Equipment:

Irradiation was conducted with a 250 kV Pantak X-ray machine (Model: HF320, Brandford, CT, USA) at a dose rate of 168 cGy /minute and a constant current of 12.5 mA. The gels were electrophoresed in a Hoefer UVT running tray (Model: HE 42-10) and Hoefer Horizontal electrophoresis Unit (Model: HE33) both manufactured by Hoefer Scientific Instruments (San Francisco, CA, USA). The comets were visualized with an Olympus fluorescence microscope (model: Olympus BX60, DplanApo, Olympus Optical). Comet images were captured by using a Hitachi CCD Color Camera (KP-D581) and a Matrox comet card (Matrox Electronic System, Montreal, QC, Canada). The

images were analyzed by the Alkomet v2.1 image analysis system (Richard Branker Research, Ottawa, ON, Canada).

### **2.8.3 Methods**

The experiments were set up in two groups of cells comprised of an X-ray irradiated group and a non-irradiated group (control group). Both groups of cells were given a one hour cisplatin exposure, at five concentrations from 0 to 100  $\mu\text{M}$ . All experimental conditions were the same for both groups, except for the irradiated group, which was given a dose of 10 Gy of X rays, while the control group was not.

The comet assay was conducted at different time points. For the zero time points, the X-ray exposure and comet assay were conducted immediately after one hour of cisplatin treatment. For the sixteen hour time points, the cells were washed in PBS and incubated in fresh MEM for sixteen hours after the one hour cisplatin exposure, before irradiating the cells and conducting the comet assay.

For each time point,  $4 \times 10^5$  MDCK cells were seeded in each well of multiwell (6 well) dishes (Becton Dickinson, NJ, USA) and incubated for three days. The cells were exposed to cisplatin from 0  $\mu\text{M}$  to 100  $\mu\text{M}$  for one hour in the incubator. After the cells were taken out of the incubator, the medium was removed and the cells were washed three times by adding 2 ml of PBS to each well.

Trypsin was added to the cells, and they were incubated at 37°C for twenty minutes. Fresh MEM with 10% FBS was then added to prevent further digestion by

trypsin. The cells were collected, and counted under the microscope according to the method described in 2.3.2 and diluted to  $2 \times 10^5$  cells /ml in MEM.

One hour prior to the experiment, the two-well super cell chambers (Fisher Scientific, Pittsburgh, PA, USA) were detached from their glass slide mounts and re-affixed to a 10 cm x 6.5 cm piece of gel bond film (FMC Bioproducts, Rockport, ME). A 30  $\mu$ l aliquot of each diluted cell suspension was added to 270  $\mu$ l of liquid 0.75% low melt point agarose (37 °C), and gently mixed by pipetting. A 120  $\mu$ l aliquot of the cell and agarose mixture was cast in each well of a two-well Super cell chamber for each sample tested. Each sample was cast in triplicate. Once the agarose was solidified, the super cell chambers were carefully removed from the gel bond and the samples of agarose-embedded cells remained attached to the gel bond.

The gel bond films with cells attached were equilibrated in MEM with 10 % FBS for 15 minutes at 37 °C. The irradiated group was placed on ice in the chamber of the X-ray irradiator and exposed to 10 Gy, while the control group was placed on ice in the dark at the same time. Immediately, the gels were placed in 50 ml ice-cold lysis buffer A for 30 minutes in the dark on ice. The gels were rinsed three times with distilled water, placed in 40 ml of lysis buffer B containing 1mg/ml of proteinase K, incubated at 37°C in the dark for 60 minutes, and washed three times in distilled water. After the gels were placed in 50 ml electrophoresis buffer for 30 minutes, each gel was placed in a Hoefer UVT running tray in a Hoefer Horizontal electrophoresis unit containing 220 ml of electrophoresis buffer. The electrophoresis was run at 300 mA per gel and at about 19 V for 20 minutes. Finally, The gels were rinsed once with distilled water, and placed in 50

ml of 1 M ammonium acetate solution for 30 minutes, rinsed again with distilled water and placed in absolute ethanol overnight before air drying.

After drying, agarose-gelbond films were cut into 20 mm x 25 mm strips and stained for 20 minutes with SYBR Gold (1/10,000 dilution of stock solution, 495 nm excitation, 537 nm emission). The agarose-gelbond films were then rinsed with distilled water and placed on glass slides. A 50 x 22 mm glass cover slip was applied and firmly but gently pressed onto the gel, removing excess water and forming a tight seal.

Comets in the gels stained with SYBR gold were visualized under the above mentioned fluorescence microscope at 40 X by using an "IB" cube. Fluorescence-stained comet images were captured with a Hitachi CCD color Camera. Images were analyzed by the Alkomet v2.1 image analysis system from Richard Branker Research. For each sample, a minimum of 55 cells were simultaneously scored for tail length, and tail moment.

### **3. Results**

#### **3.1 Growth Curve of MDCK Cells**

The growth curve of MDCK cells in MEM medium with 10 % FBS is presented in Figure 3.1. The medium was not changed during the eleven days. After  $1.5 \times 10^6$  cells were seeded on day zero, the cells reached the plateau phase at day four. The straight portion of the growth curve indicating the cells growing in the log phase were used by Prism™ statistical software (GraphPad Software Inc., San Diego, CA, USA) for the calculation of doubling time. The doubling time of MDCK cells in MEM with 10 % FBS is about  $40 \pm 5$  hours (SD).

### Growth Curve of MDCK Cells

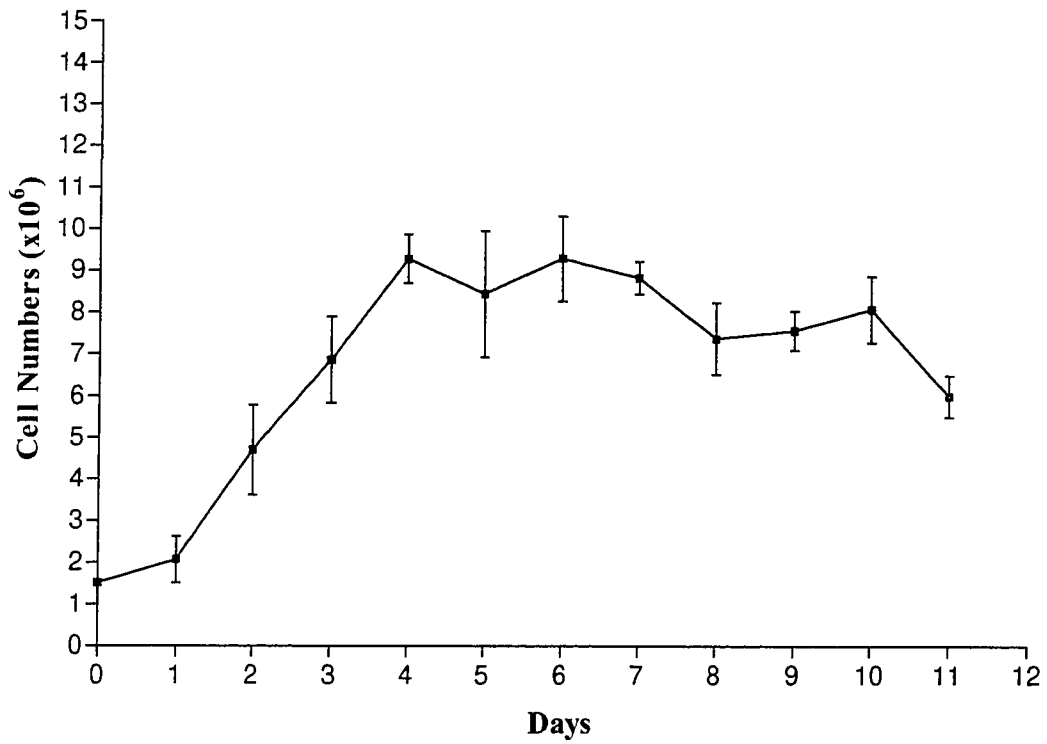


Figure 3. 1 The error bars represent standard deviation around the mean (n=3).

### **3.2 Cisplatin-induced Cytotoxicity Measurement**

Cells at the late exponential phase (day 3) were harvested from 5 cm petri dishes. The response of these cells to cisplatin was determined by seeding 1000 cells for the control, while 5000 cells were seeded for the drug treated cells as described in section 2.4.2. The concentrations of cisplatin were 0, 5, 15, 25, 50, 75, and 100  $\mu\text{M}$ . After ten days of undisturbed exposure to MEM with 10 % FBS, colonies were processed and counted as described in section 2.4.2.

The percentage of colonies of MDCK cells formed after exposure to different concentrations of cisplatin compared to their matched control is presented in Figure 3.2. The  $\text{IC}_{50}$  of cisplatin in MDCK cells is  $17 \mu\text{M} \pm 5 \mu\text{M}$  (SD). The plating efficiency is about  $16\% \pm 3\%$  (SD).

### Cisplatin Dose-Response Curve

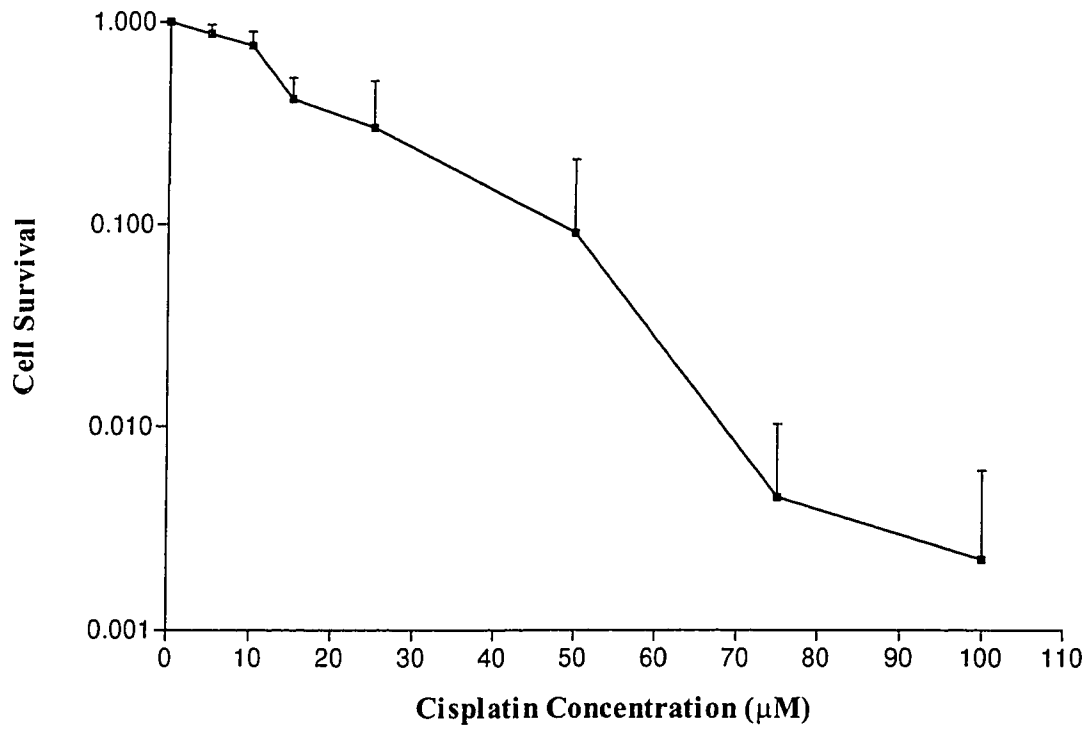


Figure 3. 2 The error bars represent standard deviation around the mean (n = 4).

### 3.3 Cellular Accumulation of Platinum

The intracellular accumulation of platinum in MDCK cells after a one hour exposure to cisplatin is represented in Figure 3.3. Cisplatin cellular accumulation was assayed by exposing monolayer cells in 5 cm petri dishes to cisplatin at concentrations of 0, 50, 75, and 100  $\mu\text{M}$ . The exposure concentrations were selected based upon the toxicity range of cisplatin in MDCK cells and the detection limit of the atomic absorption spectrophotometer. The lowest extracellular cisplatin concentration that leads to a detectable level of cisplatin is 50  $\mu\text{M}$ . The  $\text{IC}_{100}$  of cisplatin in MDCK cells is 100  $\mu\text{M}$ . The detection limit of cisplatin by atomic absorption spectrophotometry is 50 ng/ml.

Platinum accumulation in MDCK cells is reported as ng of platinum per million cells. The regression curve of platinum uptake in MDCK cells was created by Prism<sup>TM</sup> statistical software (GraphPad Software Inc., San Diego, CA, USA), which indicates that platinum accumulation in cells has a linear relationship with the exposure concentration, within the detectable concentration range of 0  $\mu\text{M}$  to 100  $\mu\text{M}$ . The  $r^2$  value is 0.94.

### Cellular Uptake of Pt after One Hour Exposure

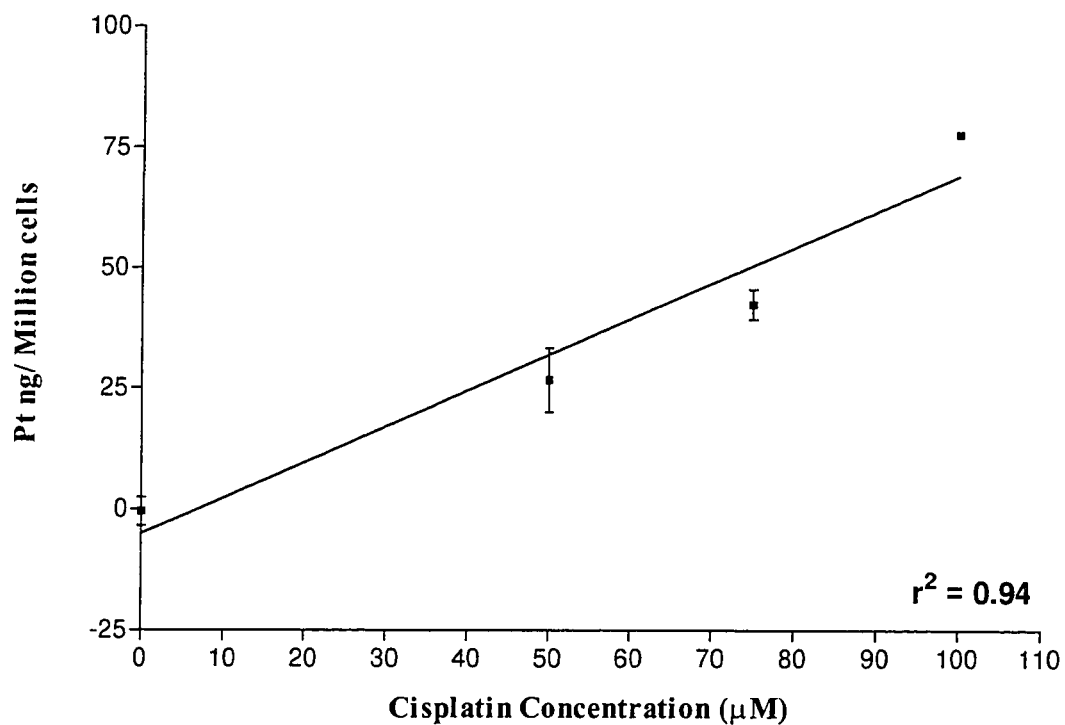


Figure 3.3 The regression curve of platinum accumulation in MDCK cells after a one hour exposure to cisplatin. The error bars represent standard deviation around the mean (n=3).

### 3.4 Platinum Binding with DNA

The relationship between the platinum bound to DNA versus the cisplatin exposure concentrations was determined. Ideally for this experiment, we would have used the cisplatin dose range used in the clonogenic assay. Unfortunately, the platinum detection limit of atomic absorption spectrophotometry (50 ng/ml) was not low enough to permit use of the clonogenic assay cisplatin dose range for these experiments. Various methods were tested in an attempt to overcome this problem, such as increasing cell numbers, increasing injection volume for atomic absorption, or using a more sensitive instrument. However, the only method that proved successful in detecting DNA-bound platinum was to increase the exposure concentration.

The exposure concentrations of cisplatin ranged from the detection limit of cisplatin (i.e. 1.5 mM) up to the maximal concentration at which cisplatin can be dissolved in saline (i.e. 3.33 mM or 1 mg/ml). MDCK cells were exposed to cisplatin at 0, 1.5, 2, and 3 mM in triplicate for one hour. For each sample, the injection into the atomic absorption spectrophotometer was conducted in triplicate.

The results for three independent experiments are presented in Figure 3.4. The quantity of platinum bound to DNA is expressed as ng platinum bound per  $\mu\text{g}$  with DNA. The regression curve indicates platinum binding with DNA has a linear relationship with cisplatin concentration from 0 mM to 3 mM. The  $r^2$  value is 0.99.

## Pt Binding with DNA

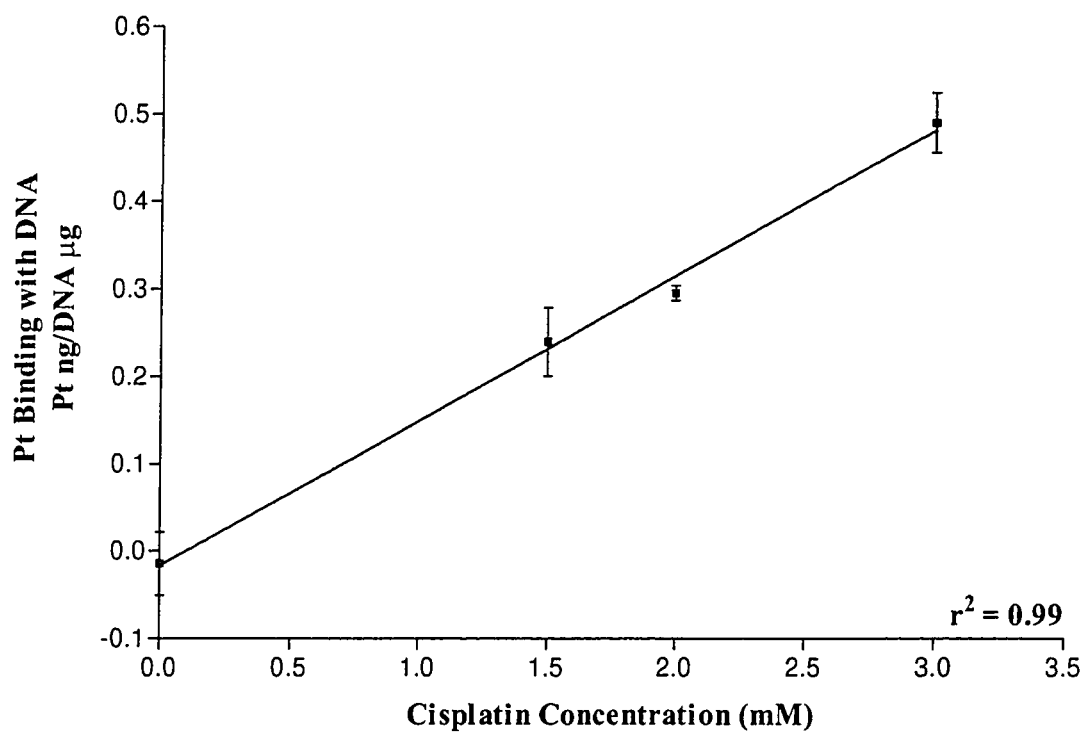


Figure 3.4 The regression curve of platinum binding with DNA versus corresponding cisplatin concentrations. The error bars represent standard deviation around the mean (n = 3).

### 3.5 Cisplatin-induced DNA Synthesis Inhibition

In order to detect whether platinum binding to DNA inhibits the synthesis of DNA, BrdU incorporation into DNA was assessed by monoclonal antibodies. MDCK cells were exposed for one hour to cisplatin in MEM without FBS at concentrations ranging from 0  $\mu\text{M}$  to 100  $\mu\text{M}$ . The cisplatin concentration range was used since it matched the cisplatin dose range used in cytotoxicity studies. Clinical cisplatin was diluted in 0.9% saline to achieve the required concentrations.

Fluorescence microscopy images of MDCK cells are presented in Figure 3.5. The figure compares control cells to cells treated with cisplatin 25  $\mu\text{M}$ . The nuclei of both control and drug treated cells were stained with Hoechst, which shows a blue color under a fluorescence microscope, representing the whole population of the cells. The secondary antibody (anti-mouse Ig) conjugated with fluorescein (FITC) against anti-BrdU (mouse monoclonal antibody) show a green color, and indicates BrdU incorporation into actively synthesized DNA.

Figure 3.6 represents the percentage of cells labeled with BrdU at different cisplatin concentrations. With an increasing cisplatin concentration, the percentage of cells actively synthesizing DNA decreased ( $P < 0.0001$  by ANOVA).

The correlation between percentage of cells labeled with BrdU and cell survival is presented in Figure 3.7. There is a linear relationship between cell survival and the percentage of DNA synthesis caused by cisplatin exposure to MDCK cells. The calculation by Prism<sup>TM</sup> statistic software (GraphPad Software Inc., San Diego, CA, USA) indicates the  $r^2$  value is 0.97.

## Immunofluorescence Microscopy of MDCK Cells

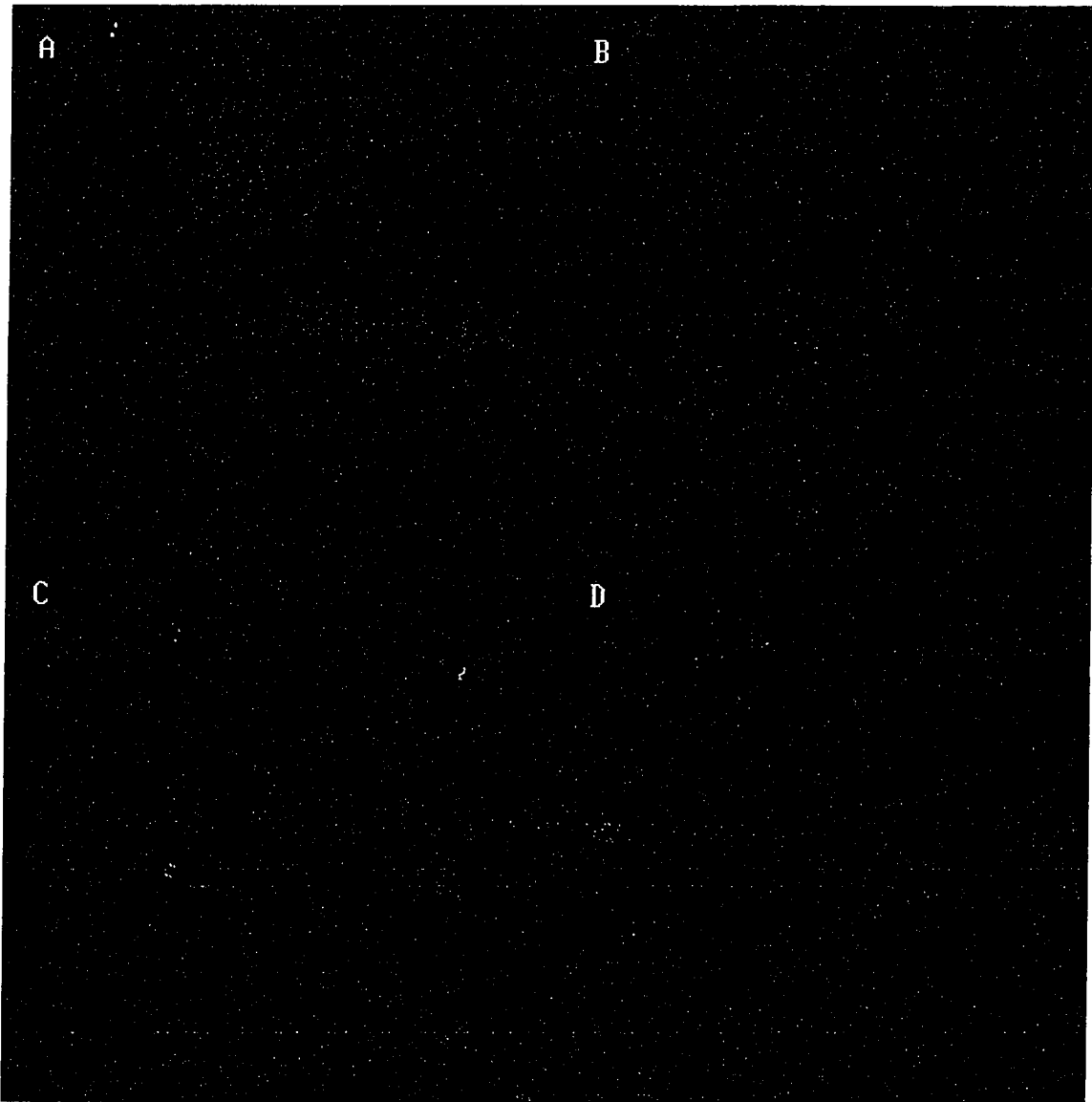


Figure 3. 5

A: Control cells, nuclei stained with Hoechst

B: Control cells, actively synthesized DNA stained with anti-mouse-Ig-fluorescein

C: Cells exposed to 25  $\mu$ M cisplatin (1 hour), nuclei stained with Hoechst

D: Cells exposed to 25  $\mu$ M cisplatin (1 hour), actively synthesized DNA stained with anti-mouse-Ig-fluorescein

### Percentage of Cells Labeled with BrdU after One Hour Cisplatin Exposure

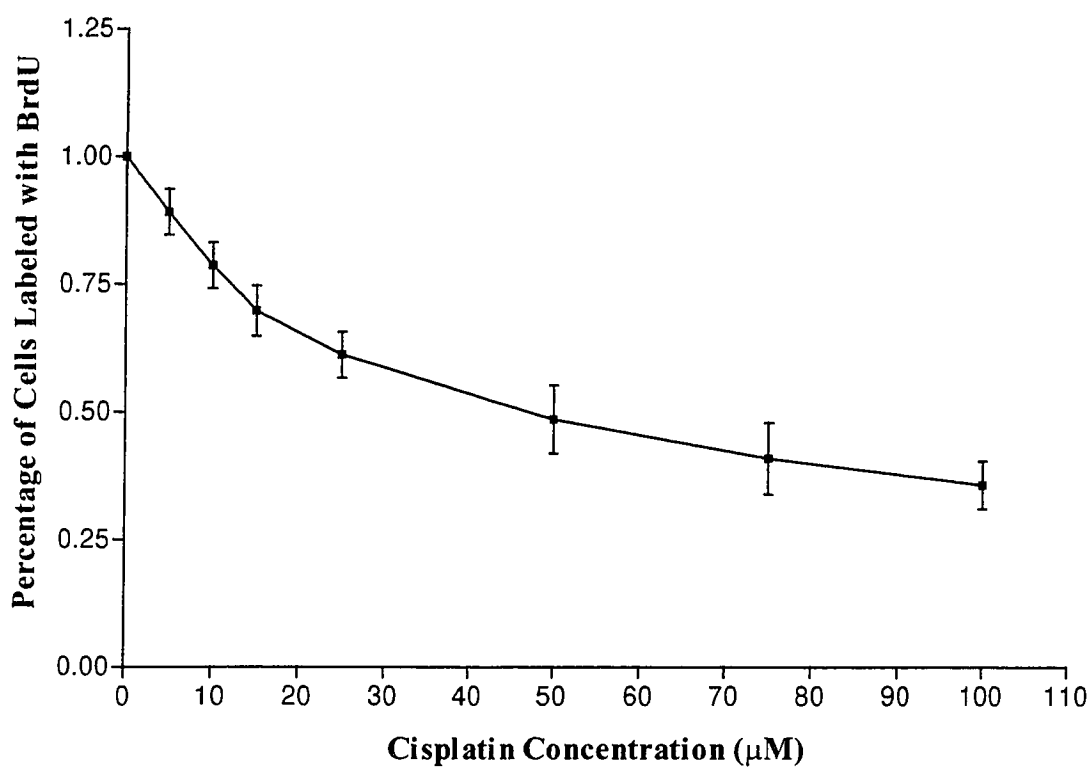


Figure 3. 6 The percentage of cells labeled with BrdU of the whole population of cells with increasing cisplatin concentration compared with control. The error bars represent standard deviation around the mean (n = 3).

### Correlation of Percentage of Cells Labeled with BrdU and Cell Survival

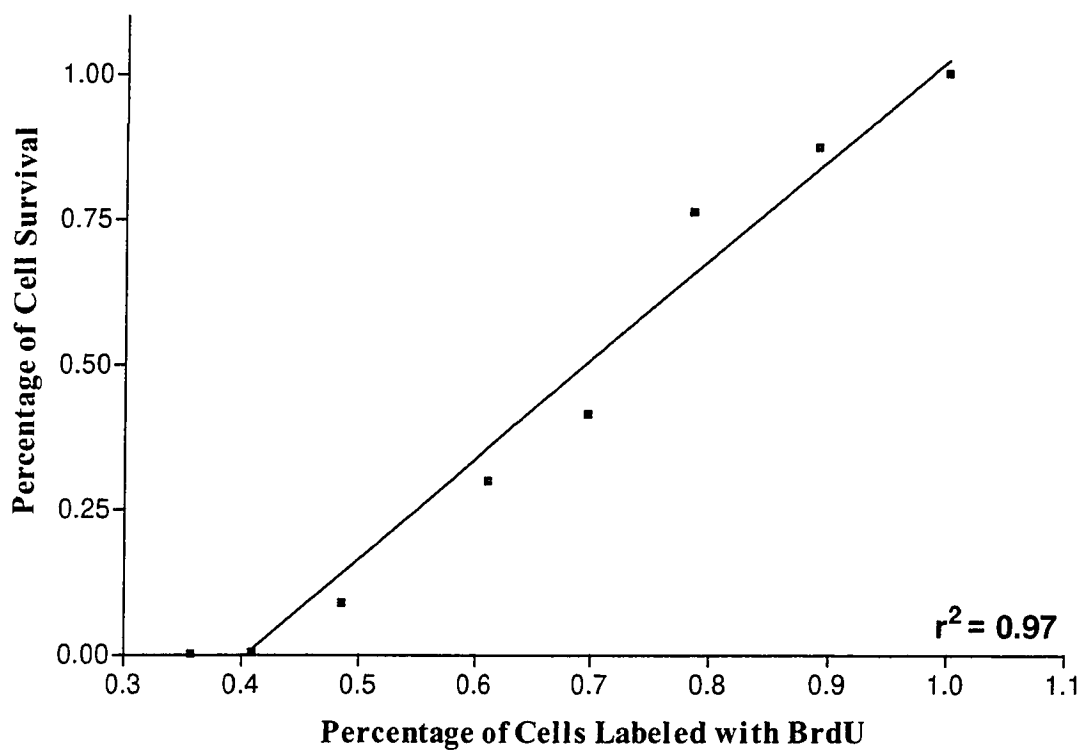


Figure 3. 7 The correlation between the percentage of cell survival and the percentage of cells labeled with BrdU of whole cell population at the corresponding cisplatin concentrations. Each point represents the mean of three independent experiments (n=3).

### 3. 6 Cisplatin-induced Pt-DNA Interstrand Cross-links

DNA-bound platinum could not be detected by atomic absorption spectrophotometry in cisplatin concentrations range used for clonogenic assays in MDCK cells. Therefore, the alkaline comet assay was used to measure platinum induced DNA interstrand cross-links. MDCK cells were exposed to cisplatin over the same concentration range used for clonogenic assays, from IC<sub>0</sub> (0 μM) to IC<sub>100</sub> (100μM).

X-ray radiation caused DNA single strand breaks, and the negatively charged pieces of broken DNA migrated in the electrophoresis field toward the anode after the individual cells were lysed. This migration was visualized under a fluorescence microscope as a “tail of the comet”. Since platinum formed interstrand cross-links between the two opposite strands, the migration of the broken pieces of DNA were inhibited by the Pt-DNA interstrand cross-links. Cells with platinum interstrand cross-links showed shorter tails compared with the cells without platinum interstrand cross-links.

After the MDCK cells were exposed to cisplatin for one hour, the experiments were conducted at two different time points. The experiments at the zero hour time point were conducted by irradiating the cells right after the one hour cisplatin exposure and immediately performing the alkaline comet assay. The experiments at the sixteen-hour time point were conducted by washing the cells with PBS and adding MEM with 10 % FBS immediately after the one hour cisplatin exposure. After sixteen hours of incubation, the cells were irradiated and the alkaline comet assay was immediately performed.

The experiments were set in two groups as described in section 2.8.3. The tail moments shown on the following graphs were calculated by the tail moments of the irradiated group minus the tail moments of the non-irradiated group (control group). Figure 3.8 represents the reduction of tail moments versus cisplatin exposure concentration for the zero and sixteen-hour time point experiments respectively. The tail moment is inversely related to the amount of Pt-DNA interstrand cross-links (Fairbairn et al., 1995). The results represent the average of three independent experiments for each time point.

Statistical analysis by one-way analysis of variance (ANOVA) indicates that the reduction of the tail moment with increasing cisplatin concentrations (0-100  $\mu\text{M}$ ) is statistically significant at both the zero hour ( $p=0.0049$ ) and sixteen hour ( $p= 0.0001$ ) time points. For each cisplatin concentration, the reduction in tail moment was compared by t test for the zero time points versus the sixteen hour time point. At low cisplatin concentrations (0, 10, and 25  $\mu\text{M}$ ), there was no significant difference for the two different time points with respect to reduction in the tail moment, but the two time points did differ significantly ( $p<0.05$ ) at higher cisplatin concentrations (50  $\mu\text{M}$  and 100  $\mu\text{M}$ ) points.

The percentage of the tail moment for the same experiment at the zero and sixteen hour time points is presented in Table 3.1. The controls were considered to be one hundred percent. The percentages of the tail moments of cisplatin treated cells were compared to the control. Statistical analysis by ANOVA indicates that the percentage of reduction of tail moments for both of zero and sixteen hour time points with increasing cisplatin concentrations is statistically significant ( $P < 0.0001$ ).

To determine if Pt-DNA interstrand cross-links may be related to inhibition of DNA synthesis and cell survival, correlations between the percentage of cells labeled with BrdU and the percentage of the tail moment at the corresponding cisplatin concentrations were performed. Figure 3.9 represents the correlation between the percentage of cells labeled with BrdU and the percentage of tail moment at the corresponding cisplatin concentration for the zero hour time point. The  $r^2$  value is 0.95.

In order to determine if Pt-DNA interstrand cross-links may be related to cell survival, correlations between the percentage of cell survival and percentage of tail moment were conducted. Figure 3. 10 and Figure 3.11 represent the correlation between the percentage of cell survival and the percentage of the tail moment at the corresponding cisplatin concentrations for both the zero and sixteen hour time points, respectively. The  $r^2$  value is 0.84 for the zero hour time point and 0.81 for the sixteen hour time point.

### Reduction of Tail Moment after Cisplatin Exposure (at zero and sixteen hour time points)

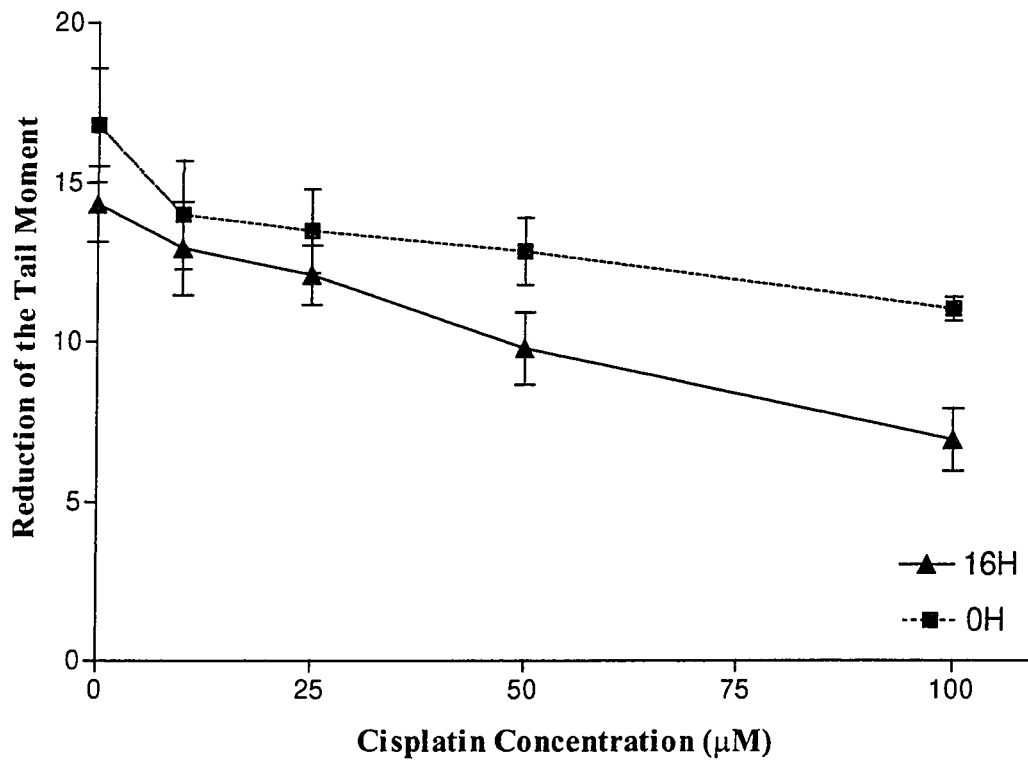


Figure 3. 8 The comparison of tail moment at the zero and sixteen hour time points after cisplatin exposure. The tail moment is inversely related to the amount of platinum DNA interstrand cross-links. The error bars represent the standard deviation around the mean (n = 3).

Cisplatin Concentrations ( $\mu\text{M}$ )	0 Hour Time Point		16 Hour Time Point	
	Percentage of Tail Moment	Standard Deviation	Percentage of Tail Moment	Standard Deviation
0	100	0	100	0
10	84	5	90	4.8
25	80	5	84	7.3
50	76	6.7	69	11.8
100	66	4.4	49	9.6

Table 3.1 The comparison of the percentage of tail moment at the zero hour and sixteen hour time points. The comet assay was conducted after a one hour cisplatin exposure at zero and sixteen hour time points (n =3).

### Correlation of Percentage of Cells Labeled with BrdU and Percentage of Tail Moment (at zero hour time point)

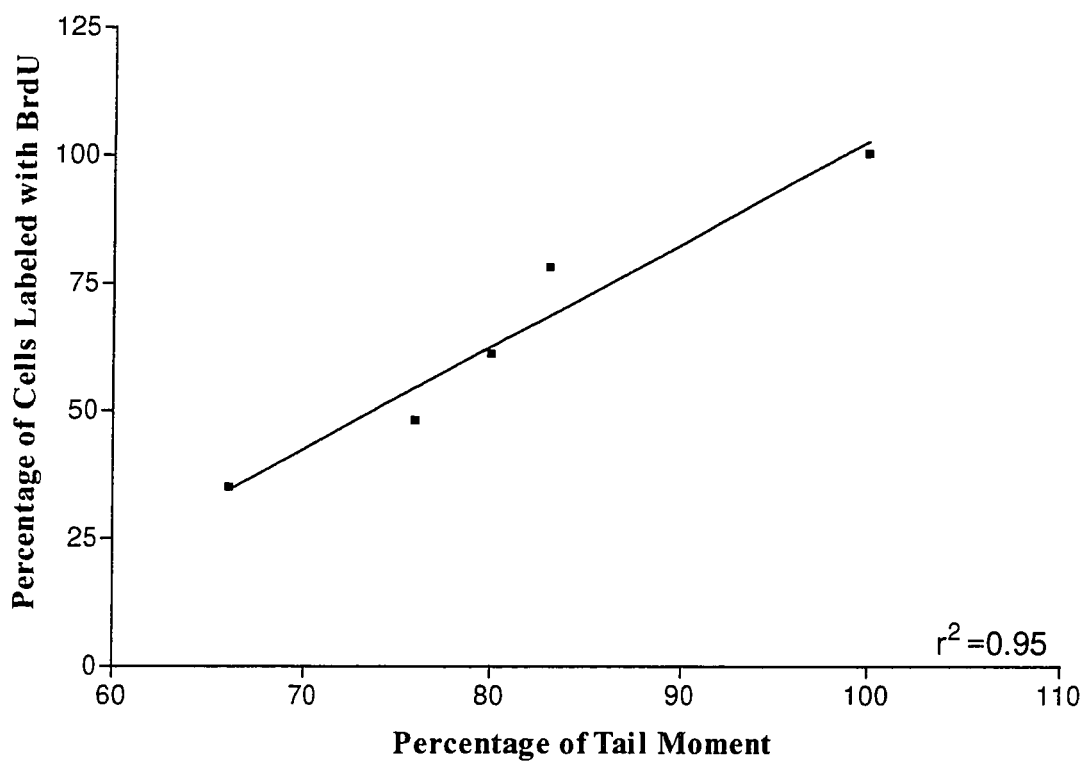


Figure 3.9 The tail moment is inversely related to the amount of platinum DNA interstrand cross-links. Each end point represents the mean of three independent experiments (n=3).

### Correlation of Percentage of Cell Survival and Percentage of Tail Moment (at zero hour time point)

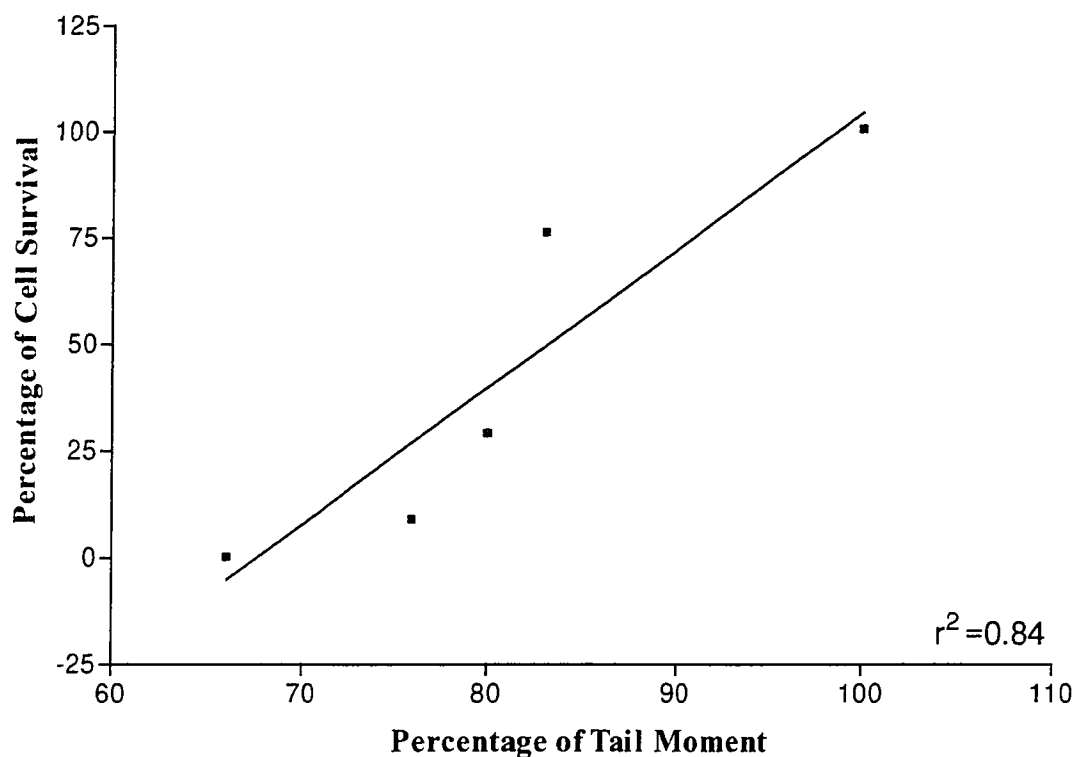


Figure 3. 10 The correlation between the percentage of the tail moment at the zero hour time point and the percentage of cell survival after a one hour cisplatin exposure. Each point represents the mean of three independent experiments (n=3).

### Correlation of Percentage of Cell Survival and Percentage of Tail Moment (at sixteen hour time point)

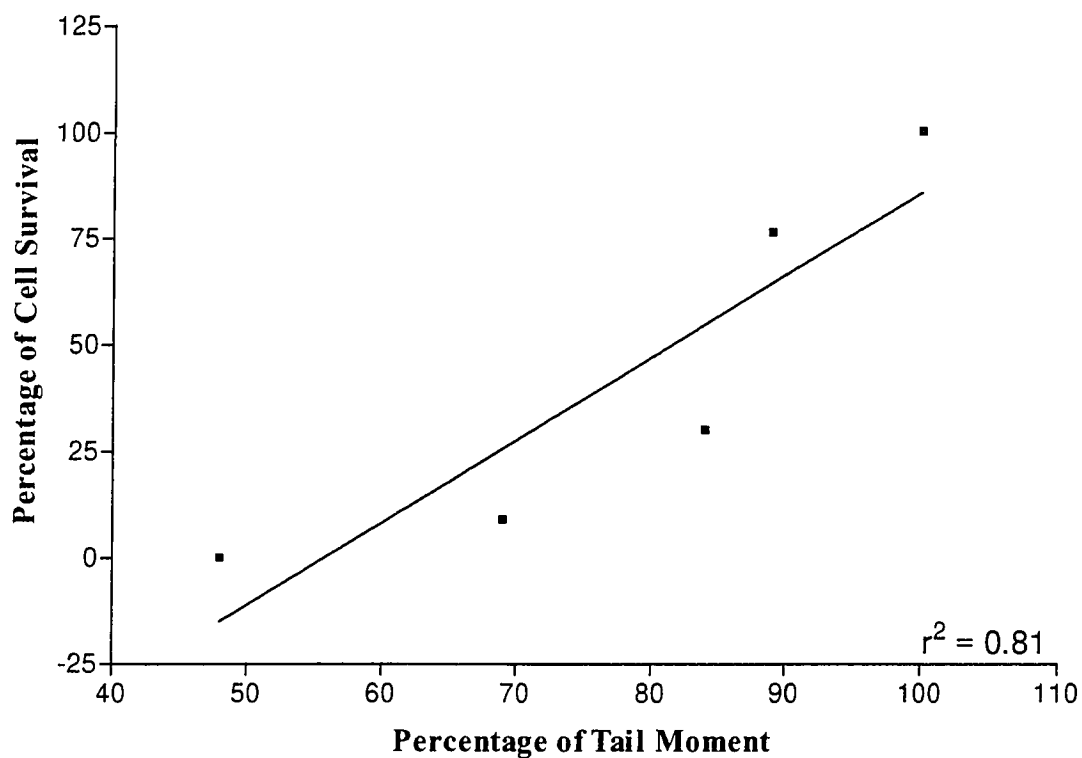
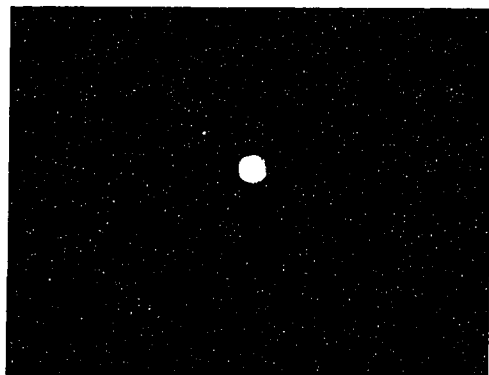


Figure 3. 11 The correlation between percentage of tail moment at the sixteen hour time point and the percentage of cell survival after a one hour cisplatin exposure. The tail moment is inversely related to the amount of platinum DNA interstrand cross-links. Each end point represents the mean of three independent experiments (n=3).

**Fluorescence-stained Comet Image for the Experiment at Zero Hour Time Point**



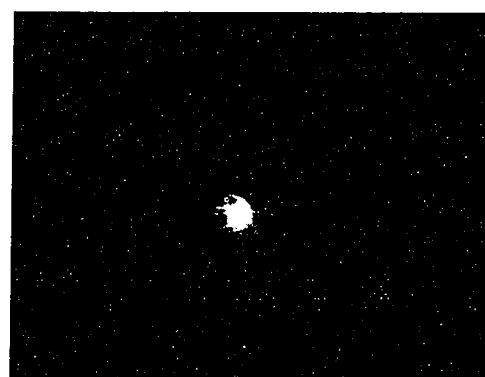
A



B



C



D

Figure 3.12 The “comet” of individual lysed cells after alkaline comet assay at the zero time point.

A: 0 Gy radiation and 0  $\mu\text{M}$  cisplatin

B: 10 Gy radiation and 0  $\mu\text{M}$  cisplatin

C: 0 Gy radiation and 100  $\mu\text{M}$  cisplatin

D: 10 Gy radiation and 100  $\mu\text{M}$  cisplatin

### Fluorescence-stained Comet Image for the Experiment at Sixteen Hour Time Point

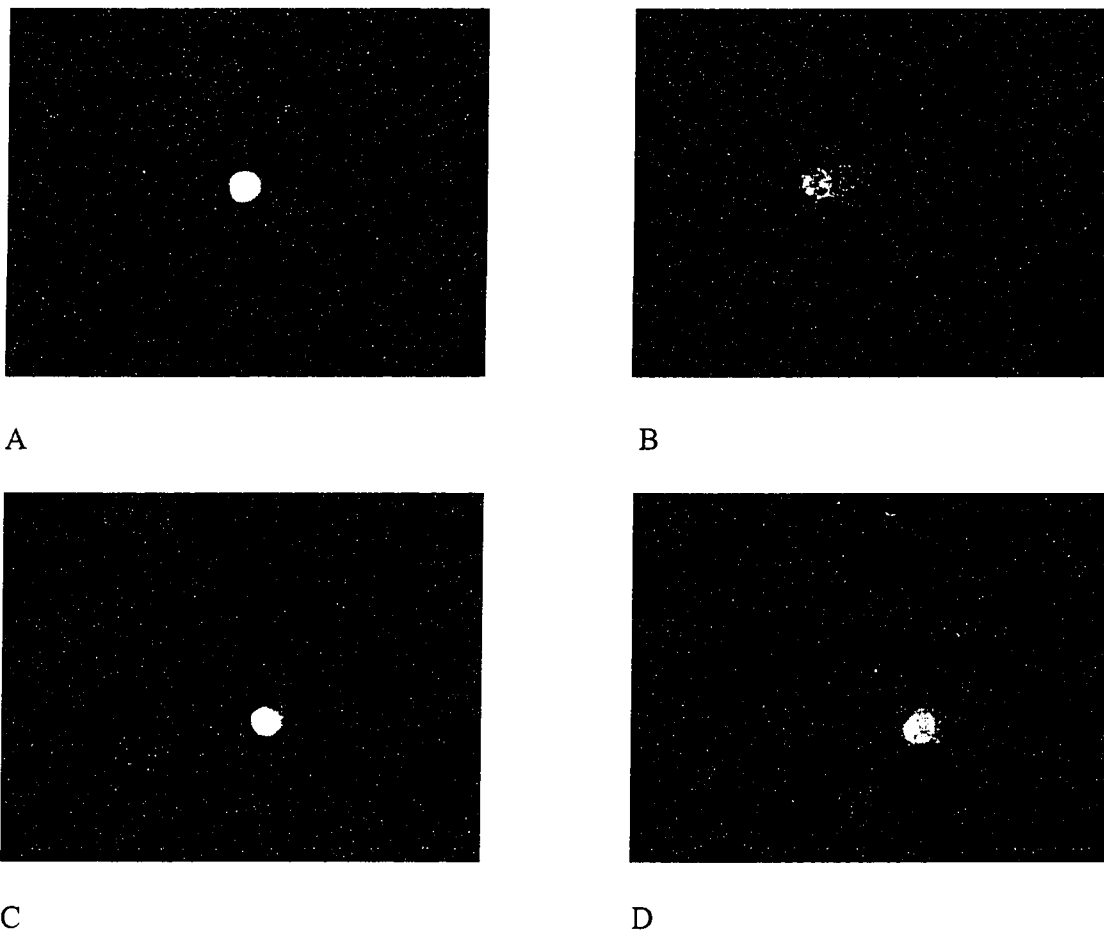


Figure 3.13 The “comet” of individual lysed cells after alkaline comet assay at the sixteen hour time point.

A: 0 Gy radiation and 0  $\mu$ M cisplatin

B: 10 Gy radiation and 0  $\mu$ M cisplatin

C: 0 Gy radiation and 100  $\mu$ M cisplatin

D: 10 Gy radiation and 100  $\mu$ M cisplatin

#### **4. Discussion:**

The mechanism of cisplatin-induced cytotoxicity in cancer cells is believed to involve DNA as a major target, with which it forms interstrand and intrastrand cross-links, but the mechanism of cisplatin-induced nephrotoxicity in humans is still not well understood (Johnson et al., 2001). Previous research indicates that the majority of cisplatin-induced renal damage is located in the proximal tubule, but the distal tubule also appears to be affected in both human and animal studies (Pinzani et al., 1994). The principle focus of this research project was to examine the effects of cisplatin on DNA and the correlation between these various effects by using MDCK cells as a an *in vitro* model of cisplatin-induced nephrotoxicity in distal tubules.

Cisplatin causes acute and cumulative chronic renal toxicity associated with histological renal damage in both humans and animals. Cisplatin administration causes impairment of proximal tubular reabsorption, but distal tubular function also seems to be affected (Pinzani et al., 1994). Tubular necrosis was observed under the electron microscope in the location of both proximal and distal tubules at three weeks after cisplatin administration in humans. Although the histological changes were most pronounced within the proximal tubule, they were observed in the distal tubular epithelium as well (Dentino et al., 1978).

*In vitro*, the LLC-PK<sub>1</sub> cell line has been used to investigate cisplatin-induced cytotoxicity in the proximal tubule. Relatively, there was more inhibition of DNA synthesis than RNA and protein synthesis by cisplatin (Montine et al., 1988). A similar phenomenon was observed by Tay et al. in rabbit renal proximal tubular cells (Tay et al.,

1988). To my knowledge, the mechanism of cisplatin-induced cytotoxicity in distal tubular cells has not yet been thoroughly investigated.

The mechanism of cisplatin uptake into cancer cells is unknown. While some evidences favor cisplatin uptake by passive diffusion, other evidences suggest active drug transport or facilitated diffusion through gated ion channels (Gately et al., 1993). This research project demonstrated that platinum accumulation in MDCK cells after a one hour exposure was proportional to the detectable extracellular concentrations of cisplatin (within the concentration range of cisplatin exposure used in our experiments). The results of this project do not provide any indication as to whether the mechanism of cisplatin uptake by either active or passive diffusion.

It is generally accepted that DNA is the target responsible for the cytotoxic action of cisplatin against cancer cells (Zwelling et al. 1980; Roberts et al., 1986; Hanušovská et al., 1987). There are reports that DNA may also be the target for the action of cisplatin against renal tubular cells. Yasumasu et al. reported that platinum binding with DNA in the renal tissue isolated from rat cortex and medulla can be detected one hour after cisplatin infusion at a concentration of 6.5 mg/kg. Their results suggested that platinum bound to DNA might be related to cisplatin-induced nephrotoxicity in rats (Yasumasu et al., 1992). In these rats, cisplatin suppressed the synthesis of nuclear DNA *in vivo* at eight, twelve and twenty four hours after injection. In addition, DNA synthesis in nuclei of renal cortical and outer medullary cells isolated from untreated rats was markedly suppressed after incubation with 10 to 25  $\mu\text{M}$  of a one hour cisplatin exposure *in vitro*. These above results indicated that cisplatin affects the synthesis rate of nuclear DNA of renal tubular cells (Yasumasu et al., 1992).

Although platinum binding with DNA showed a linear relationship with cisplatin concentrations at the supracytotoxic level in this research project, this characteristic may be different at cytotoxic concentrations. This relationship does not prove whether or not platinum binds with DNA in MDCK cells, nor does it prove that this degree of Pt-DNA binding affects the function of DNA in MDCK cells. Therefore, this research project examined the ability of cisplatin to interfere with DNA synthesis in MDCK cells *in vitro*. It was observed that cisplatin inhibited DNA synthesis in MDCK cells after a one hour exposure at a concentration as low as 10  $\mu$ M, and this inhibition was strongly correlated with cell survival. The results of this project suggest that cisplatin-induced DNA synthesis inhibition is a factor contributing to cisplatin-induced cytotoxicity in MDCK cells.

It is well known that platinum forms different adducts with DNA in cancer cells; more than 95% of the cross-links were found to be intrastrand in nature in CHO cells, and these intrastrand cross-links were determined to be responsible for cisplatin-induced cytotoxicity. Although only about 5% of platinum DNA cross-links are of the interstrand type, these cross-links are also considered to contribute to the cytotoxicity of cisplatin (Johnson et al., 2001).

Other researchers also investigated the formation of platinum DNA intrastrand cross-links after administration of cisplatin to rats. Cisplatin was given to Sprague-Dawley rats at doses of 8 mg/kg by i.v. injection. The platinum DNA intrastrand adducts from isolated normal rats kidney were detected as early as four hours after drug administration. The intrastrand adducts reached peak concentrations in renal tissue at day

two, and they persisted at detectable concentrations for fourteen days after injections (Poirier et al., 1992).

In this research project, DNA interstrand cross-links in MDCK cells were measured after a one hour cisplatin exposure at the time points of zero hour and again sixteen hours after the end of exposure. According to the principle of the alkaline comet assay, the tail moment is inversely related to the amount of DNA interstrand cross-links formed by platinum with DNA. Statistical analysis indicated that the reduction of the tail moment with increasing cisplatin concentrations was significant at both the zero and sixteen hour time points at the concentrations ranging from 0  $\mu\text{M}$  to 100  $\mu\text{M}$ . The strong correlation of the inhibition of DNA synthesis with the reduction of the tail moment suggests that cisplatin interferes with DNA synthesis in these cells through its ability to form interstrand cross-links with DNA. There were strong correlations between cell survival and the reduction of tail moment at both the zero and sixteen hour time points, which suggest that the amount of platinum DNA interstrand cross-links may be a factor contributing to cisplatin-induced death in MDCK cells.

The statistical analysis demonstrated that there were no significant differences in the reduction of tail moments by comparing the tail moment at the same concentration at two different time points at low cisplatin concentrations (10  $\mu\text{M}$ , and 25  $\mu\text{M}$ ). Only at high cisplatin concentrations (50  $\mu\text{M}$  and 100  $\mu\text{M}$ ), the reduction of tail moments at the sixteen hour time point is lower than the zero hour time point, and these differences are statistically significantly different. The above observations imply that the repair of platinum cross-links may be triggered more easily at lower cisplatin concentrations than at higher ones.

In conclusion, the accumulation of platinum into MDCK cells after a one hour exposure was observed to be linearly concentration dependent in the range of cisplatin concentrations causing cytotoxicity. Platinum binding with DNA in MDCK cells was found to be dependent upon the detectable cisplatin concentrations. It was observed that cisplatin induced DNA interstrand cross-links and impaired DNA synthesis in MDCK cells. Platinum binding with DNA, forming interstrand cross-links and subsequent interfering with its synthesis is a process that may contribute to the mechanism of cisplatin-induced cytotoxicity in MDCK cells.

Although there are strong correlations between the reduction of the tail moment and the inhibition of DNA synthesis and cytotoxicity in MDCK cells, this does not prove that platinum forms interstrand cross-links with DNA in renal distal tubular cells after clinical administration, or that this is a mechanism of cisplatin-induced nephrotoxicity in humans. If cisplatin's mechanism of nephrotoxicity in humans is via its inhibition of DNA synthesis in both distal and proximal tubular cells, then one could potentially develop agents which may selectively inhibit the effects of cisplatin on DNA in human renal tubular cells. This may eventually provide the opportunity to limit cisplatin-induced nephrotoxicity in future clinical practice and improve the therapeutic index of cisplatin.

## 5. References:

Anand AJ, Bashey B. 1993. Newer insights into cisplatin nephrotoxicity. *Ann. Pharmcother* 27: 1519-1525.

Basolo F, Perason RG. 1967. Oxidation-reduction reactions. In: *Mechanisms of Inorganic Reactions*. John Wiley & Sons Inc., NY: John Wiley & Sons, Inc. Press. p 495.

Beaty RD. 1988. In: *Concepts, instrumentation and techniques in atomic absorption spectrophotometry*. Perkin-Elmer corporation. USA.

Blachley JD, Hill JB. 1981. Renal and electrolyte disturbances associated with cisplatin. *Ann Int Med* 95: 628-632.

Buamah PK, Howell A, Whitby H, Gescher A. 1982. Assessment of renal function during high-dose cis-platinum therapy in patients with ovarian carcinoma. *Cancer Chemother Pharmacol* 8: 281-284.

Buckley JE, Clark VL, Meyer TJ, Pearlman W. 1984. Hypomagnesemia after cisplatin combination chemotherapy. *Arch Inter Med* 144: 2347-2348.

Compendium of pharmaceuticals and specialties (CPS), Thirty-sixth Edition, 2001. 1210-1212.

Daugaard G, Abildgaard U, Holstein-Rathlou N, Leyssac PP. 1988. Renal tubular function in patients treated with high-dose cisplatin. *Clin Pharmacol Ther.* 44: 164-172.

Delbancut A, Lagroye I, Cambar J. 1994. Renal cytotoxicity of cisplatin in cultured glomerular mesangial and proximal and distal tubular cells. *Toxic in Vitro.* 8(4): 517-519.

Dentino M, Luft FC, Yum MN, Einhorn LH. 1978. Long term effect of cis-diamminedichloride platinum (CDDP) on renal function and structure in man. *Cancer.* 41: 1274-1281.

Eastman A. 1987. The formation, isolation and characterization of DNA adducts produced by anticancer platinum complexes. *Pharmac. Ther* 34: 155-166.

Fairbairn D, Olive WPL, O'Neill KL. 1995. The comet assay: a comprehensive review. *Mutat Res* 339: 37-59.

Fichtinger-Schepman AMJ, van der Veer JL, den Hartog JHJ, Reedijk J. 1985. Adducts of the antitumor drug cis-diamminedichloroplatinum (II) with DNA: formation, identification, and quantitation. *Biochemistry* 24: 707-713.

Field MJ, Bostrom TE, Seow F, Cockayne DJH. 1989. Acute cisplatin nephrotoxicity in the rat evidence for impaired entry of sodium into proximal tubule cells. *Pflugers Arch* 414(6): 647-650.

Fjeldborg P, Sørensen J, Helkjer PE. 1986. The long-term effect of cisplatin on renal function. *Cancer* 58: 2214-2217.

Fram RJ, Woda BA, Wilson JM, Robichaud N. 1990. Characterization of acquired resistance to *cis*-Diamminedichloroplatinum (II) in BE human colon carcinoma cells. *Cancer Res* 50: 72-77

Gaffin SL. 1979. Rapid solubilization of human body tissues and tissue fluids for microdetermination of heavy metals. *Clinical Toxicol* 15: 293-300.

Gately DP, Howell SB. 1993. Cellular accumulation of anticancer agent cisplatin: A review. *Br. J. Cancer* 67: 1171-1176.

Gellert RW, Bau R. 1979. In: Sigel editor. *Metal ions in biological system*. Marcel Dekker Inc., NY: Marcel Dekker Inc. Vol. 8, Chap. 1.

Gonzalez-Vitale JC, Hayes DM, Cvitkovic E, Sternberg SS. 1977. The renal pathology in clinical trials of *cis*-platinum (II) diamminedichloride. *Cancer* 39: 1362-1371.

Goodman and Gilman. 1990. Miscellaneous agents. In: Gilman AG, Rall TW, Nies AS, Taylor P, editors. The pharmacological basis of therapeutics. Pergamon Press. p1249-1251.

Gratzner HG. 1982. Monoclonal antibody to 5-Bromo- and 5-Iododeoxyuridine: A new reagent for detection of DNA replication. *Science* 218(29): 474-475.

Hamilton TC, Lai GM, Rothenberg LM, Ozols RF. 1989. Mechanism of resistance to cisplatin and alkylating agents. In: Ozols RF, editor. Drug Resistance in Cancer therapy. Kluwer Academic Publishers, Boston: Kluwer Academic Publishers.

Hanušovská E, Ujházy V. 1987. DNA synthesis, protein synthesis and platinum content following drug administration in cis-diammine-dichloroplatinum (II)-sensitive and resistant L1210 cells transferred from *in vitro* to *in vivo* condition. *Neoplasma* 34: 721-726.

Hoeschele JD, VanCamp L. 1971. In: Miroslav H, editor. Advances in antimicrobial and antineoplastic chemotherapy. University Park Press, Baltimore: University Park Press. 2: p241-242.

Irwin N. 1989. Purification of plasmid DNA by precipitation with polyethylene glycol. In: Sambrook J, Fritsch EF, Maniatis T, editors. Molecular cloning a laboratory manual. Cold Spring Harbor, NY: Cold Spring Harbor laboratory Press. p E5

Johnson SW, Stevenson JP, O'Dwyer PJ. 2001. Cisplatin and its analogues. In: DeVita VT, Hellman S, Rosenberger SA, editors. Cancer principles & practice of oncology. Lippincott Williams & Wilkins, PA: Lippincott Williams & Wilkins Press. p376-388.

Kröning R, Katz D, Lichtenstein A, Nagami G. 1999. Differential effects of cisplatin in proximal and distal renal tubule epithelial cell lines. Br J Cancer 79(2): 293-299.

Kuhlmann MK, Burkhardt G, Köhler H. 1997. Insights into potential cellular mechanisms of cisplatin nephrotoxicity and their clinical application. Nephrol Dial Transplant 12: 2478-2480.

Lai GM, Ozols RF, Smyth JF, Hamilton TC. 1988. Enhanced DNA repair and resistance to cisplatin in human ovarian cancer. Biochem Pharmacol 37: 4597-4600

Lippard SJ. 1982. New chemistry of an old molecule: *cis*-[Pt (NH<sub>3</sub>)<sub>2</sub>Cl<sub>2</sub>]. *Science*. 218(4577): 1075-1082.

McKelvey-Martin VJ, Green MHL, Schmezer P, Collins A. 1993. The single cell gel electrophoresis assay (comet assay): A European review. *Mutat Res* 288: 47-63.

McNamee JP, Mclean JRN, Ferrarotto CL, Bellier PV. 2000. Comet assay: rapid processing of multiple samples. *Mutat Res* 466: 63-69.

Meijer S, Sleijfer DT, Mulder NH, Mandema E. 1983. Some effects of combination chemotherapy with *cis*-platinum on renal function in patients with nonseminomatous testicular carcinoma. *Cancer* 51: 2035-2040.

Miller SE, Gerard KJ, House DA. 1991. The hydrolysis products of *cis*-diamminedichloroplatinum (II) 6. A kinetic comparison of the *cis*- and *trans*- isomers and other *cis*-di(amine)di(chloro) platinum (II) compounds. *Inorganica Chimica Acta* 190: 135-144.

Mistry P, Lee V, Mcbrein DCH. 1989. Intracellular metabolites cisplatin in the rat kidney. *Cancer Chemopther Pharma* 24: 73-79.

Montine TJ, Borch RF. 1988. Quiescent LLC-PK<sub>1</sub> cells as a model for cis-diamminedichloroplatinum (II) nephrotoxicity and modulation by thiol rescue agents. *Cancer Res* 48: 6017-6024.

Nagai N, Kinoshita M, Ogata H, Kurita Y. 1996. Relationship between pharmacokinetics of unchanged cisplatin and nephrotoxicity after intravenous infusions of cisplatin to cancer patients. *Cancer Chemother Pharmacol* 39: 131-137.

O'Dwyer PJ, Johnson SW, Hamilton TC. 1996 Cisplatin and its analogues. In: DeVita VT, Hellman S, Rosenberger SA, editors. *Cancer principles & practice of oncology*. Lippincott Williams & Wilkins, PA: Lippincott Williams & Wilkins Press. p 418-432.

Olive PL. 1999. Review DNA damage and repair in individual cells: applications of the comet assay in radiology. *Int. J. Radiat. Boil* 75(4): 395-405.

Olive PL, Banáth J P, Durand RE. 1990. Heterogeneity in radiation-induced DNA damage and repair in tumor and normal cells measured using the “comet” assay. *Radiat. Res* 122: 86-94.

Pause A, Lee S, Lonergan KM, Klausner RD. 1998. The von Hippel-Lindau tumor suppressor gene is required for cell cycle exit upon serum withdrawal. *Proc. Natl. Acad. Sci* 95: 993-998.

Pinzani V, Bressolle F, Haug IJ, Balmès JP. 1994. Cisplatin-induced renal toxicity and toxicity-modulating strategies: a review. *Cancer Chemother Pharmacol* 35: 1-9.

Poirier MC, Reed E, Litterst CL, Gupta-Burt S. 1992. Persistence of platinum-amine-DNA adducts in gonads and kidneys of rats and multiple tissues from cancer patients. *Cancer Res* 52: 149-153.

Raaphorst GP, Chabot P, Doja S, Ng CE. 1996. Effect of hyperthermia on cisplatin sensitivity in human glioma and ovarian carcinoma cell lines resistant and sensitive to cisplatin treatment. *Int. J. Hyperthermia* 12(2): 211-222.

Robert JJ, Knox RJ, Friedlos F, Lydall DA. 1986. DNA as the target for the cytotoxic and antitumor action of platinum coordination complexes: comparative *in vitro* and *in vivo* studies of cisplatin and carboplatin. In: McBrien DCH, Slater TF editors. Biochemical mechanism of platinum antitumor drugs. IRL Press Limited, Oxford: IRL Press. p 29-64.

Rosenberg B, VanCamp L, Krigas T. 1965. Inhibition of cell division in *Escherichia coli* by electrolysis products from a platinum electrode. Nature 205: 698.

Rosenberg B, VanCamp L, Grimley EB, Thomson AJ. 1967. The inhibition of growth cell division in *Escherichia coli* by different ionic species of platinum (IV) complexes. J Biol Chem. 25: 1347-1967.

Rosenberg B, VanCamp L. 1969. Platinum compounds: a new class of potent antitumour agents. Nature 222: 385-386.

Rosenberg B, VanCamp L. 1970. The successful regression of large solid sarcoma 180 tumors by platinum compounds. Cancer Res 30: 1799-1802.

Saier Jr. MH, Erlinger S., Boerner P. 1982. Studies on growth regulation and the mechanism of transformation of the kidney epithelial cell line, MDCK: importance of transport function to growth. *Prog Clin Biol Res* 91: 569-597.

Salmon SE, Sartorelli AC. Cancer chemotherapy. In: Bertram G. K. editor. *Basic & clinical pharmacology*. 6th ed. Appleton & Lange. p 823-837.

Sherman SE, Lippard SJ. 1987. Structural aspects of platinum anticancer drug interactions with DNA. *Chem. Rev.* 87: 1153-1181.

Siddik ZH, Dible SE, Boxall FE, Harrap KR. 1986. Renal pharmacokinetics and toxicity of cisplatin and carboplatin in animals. In: *Biochemical mechanisms of platinum antitumor drugs*. IRL Press Limited, Oxford: IRL Press. p 171-198.

Stewart DJ, Mikhael NZ, Nanji AA, Maroun A. 1985. Renal and hepatic concentrations of platinum: relationship to cisplatin time, dose, and nephrotoxicity. *J Clin Oncol* 3(9):1251-1256.

Stewart DJ, Dulberg C, Molepo JM, R Goel. 1994. Factors affecting human autopsy kidney-cortex and kidney-medulla platinum concentrations after cisplatin administration. *Cancer Chemother Pharmacol* 34: 14-22.

Tay LK, Bregman CL, Masters BA, Williams PD. 1988. Effects of cis-Diamminedichloroplatinum (II) on rabbit kidney *in vivo* and on rabbit renal proximal tubule cells in culture. *Cancer Res* 48: 2538-2543,

Tucker MA, Colvin CB, Martin DS. 1964. Substitution reactions of Trichloroammineplatinate (II) ion and the *trans* effect. *Inorg Chem* 3(10): 1373-1383.

Yasumasu T, Ueda T, Uozumi J, Kumazawa J. 1992. Comparative study of cisplatin and carboplatin on pharmacokinetics, nephrotoxicity and effect on renal nuclear DNA synthesis in rats. *Pharmacol Toxicol* 70: 143-147.

Zwelling LA, Kohn KW. 1980. Effects of cisplatin on DNA and the possible relationships to cytotoxicity and mutagenicity in mammalian cells. In: Prestayko AW, Crooke ST, Carter SK, editors. *Cisplatin current status and new developments*. Academic Press, NY: Academic Press. p 21-35.